Extratropical Air -Sea Interaction

-atmospheric forcing of SST

-atmospheric response to SST

Regression onto leading PC of SST

Reanalysis

AGCM ensemble avg.

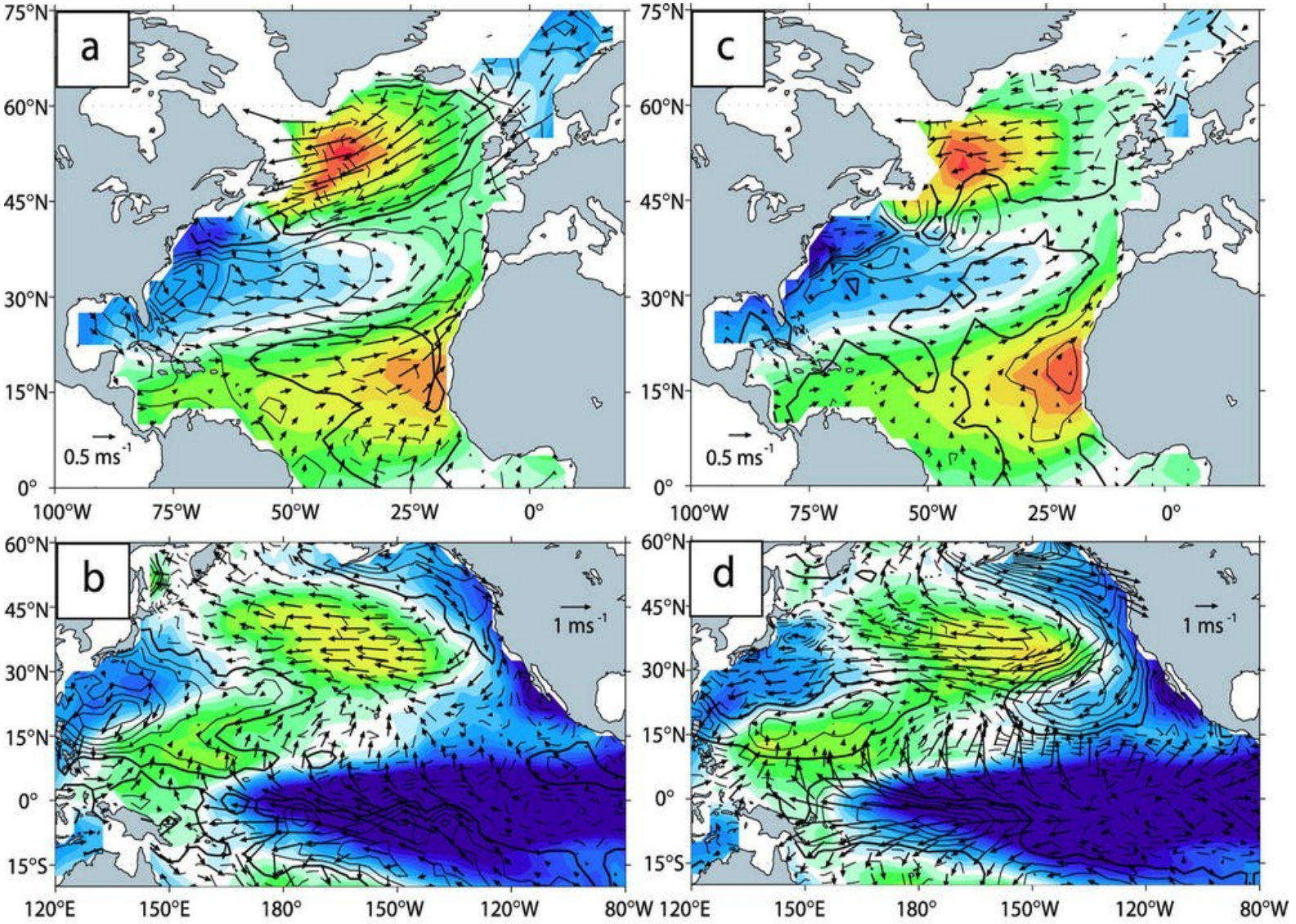

Q contours 3 Wm^{-2}

Kushnir et al. 2002

Dec-Mar air temperature and geopotential height anomalies (in m) regressed onto leading PC of North Atlantic SST. Section at 52.5N.

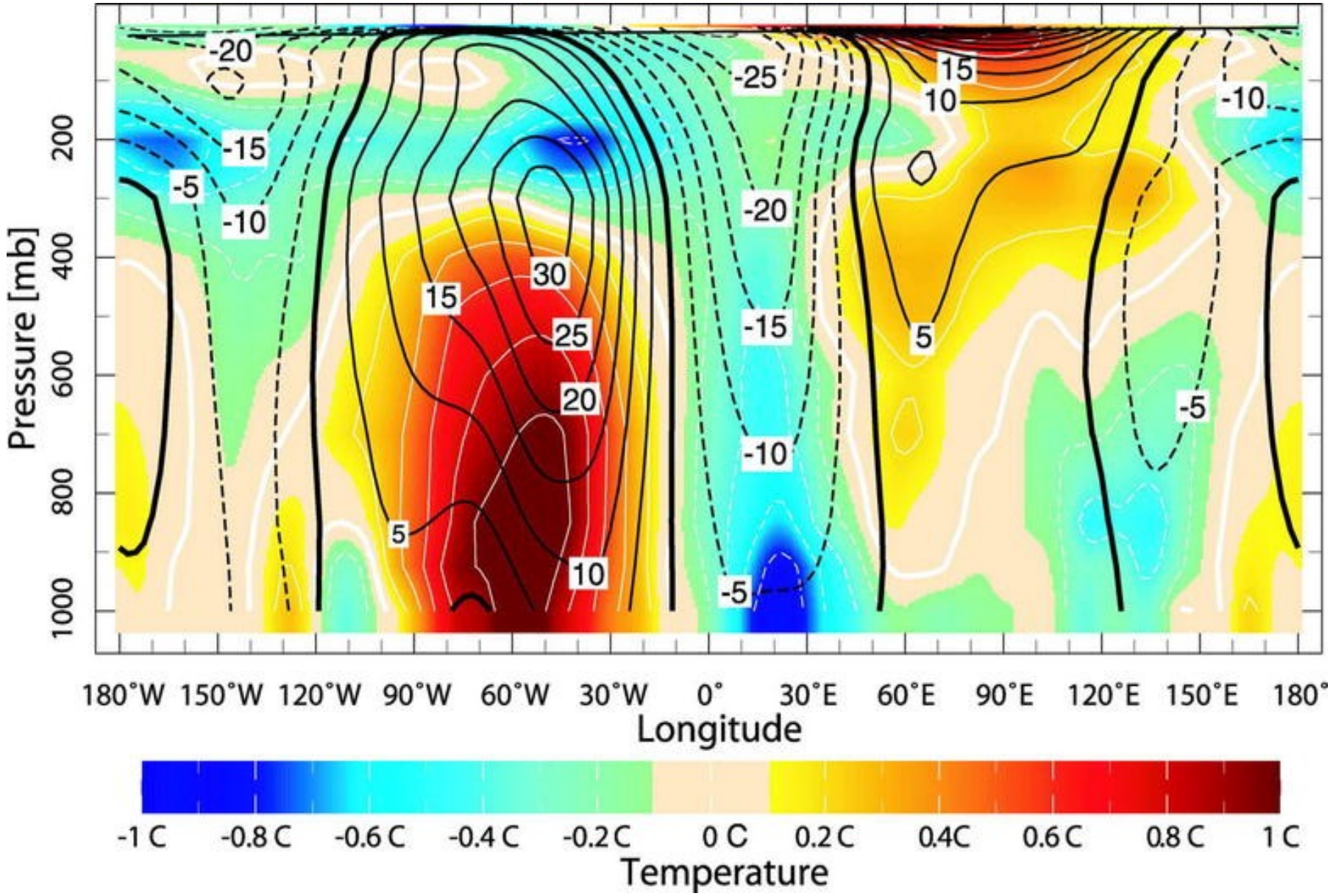

Kushnir et al. 2002

EOF of sea level pressure

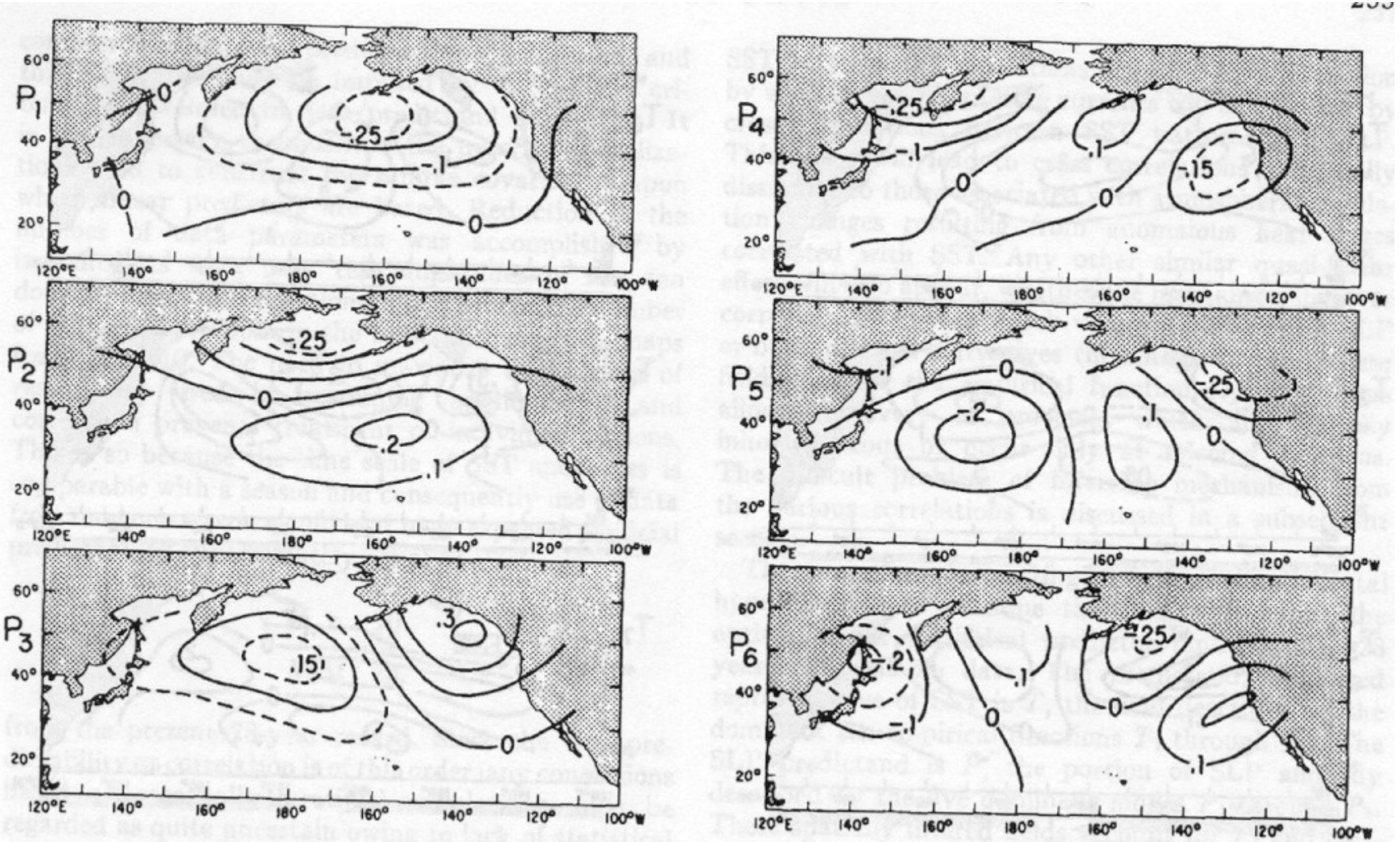

FIG. 3. The six principal empirical orthogonal functions, P_1–P_6, describing SLP anomalies.

Davis 1976

EOF of sea surface temperature

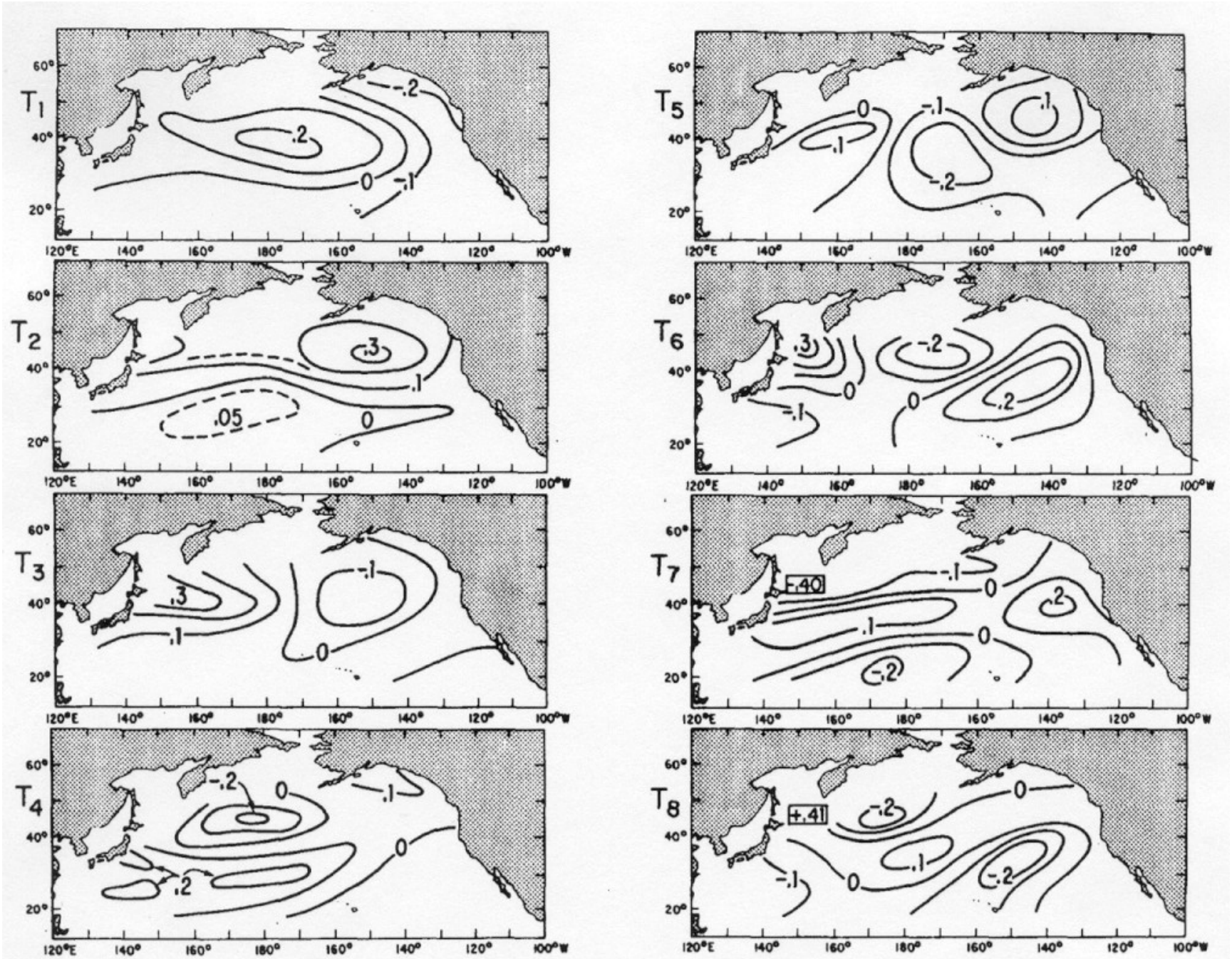

FIG. 4. The eight principal empirical orthogonal functions, T_1–T_8, describing SST anomalies.

Davis 1976

Atmosphere forces the ocean

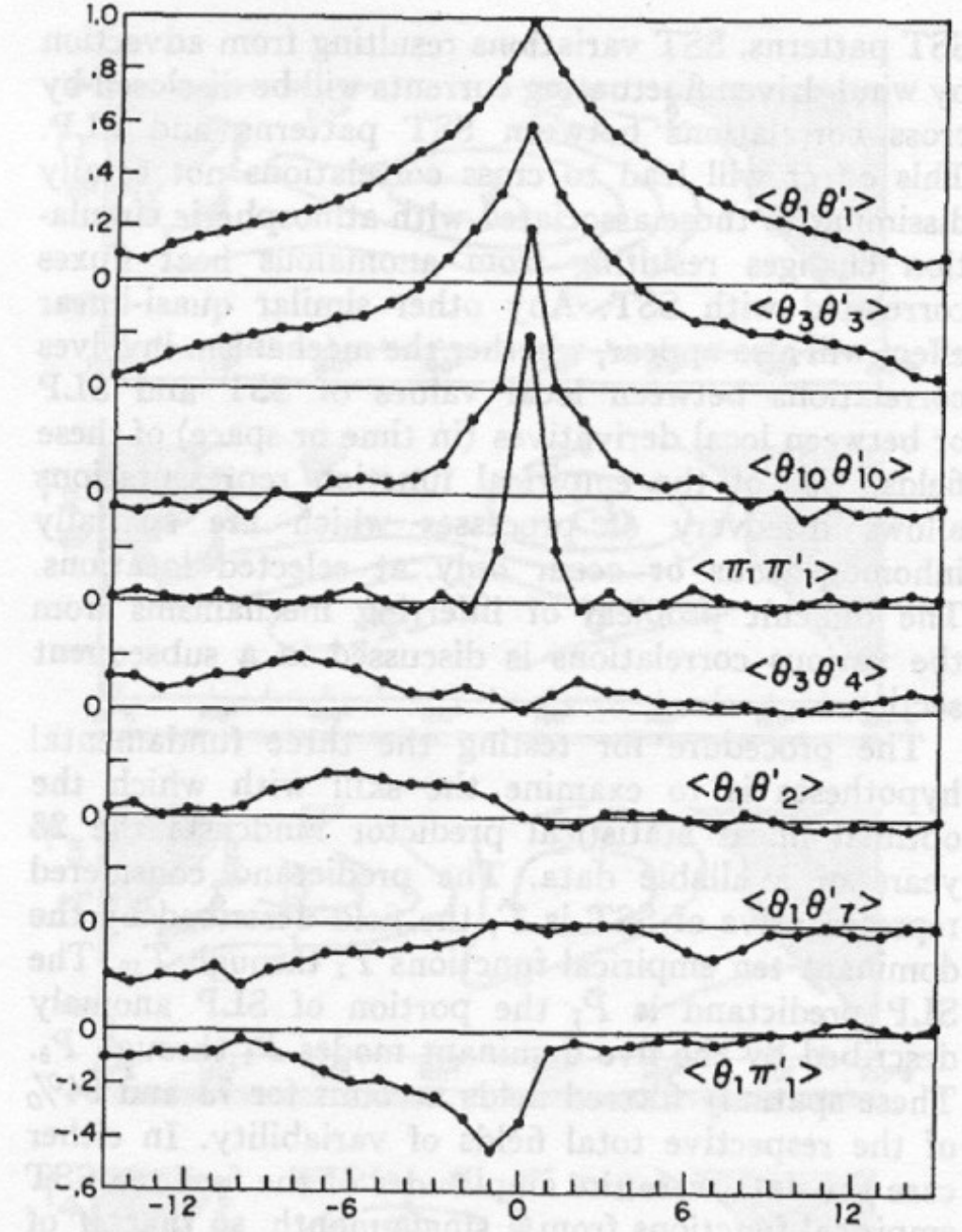

FIG. 6. Correlations between amplitudes of various SST and SLP modes. The amplitudes of SST mode n and SLP mode m are θ_n and π_m, respectively. The abscissa is the time lag t' so that the curve labeled $\langle\theta_3\theta_4'\rangle$ is the correlation of $\theta_3(t)$ and $\theta_4(t+t')$. Thus, significant correlation of π_1 and θ_1 occurs only when π_1 leads.

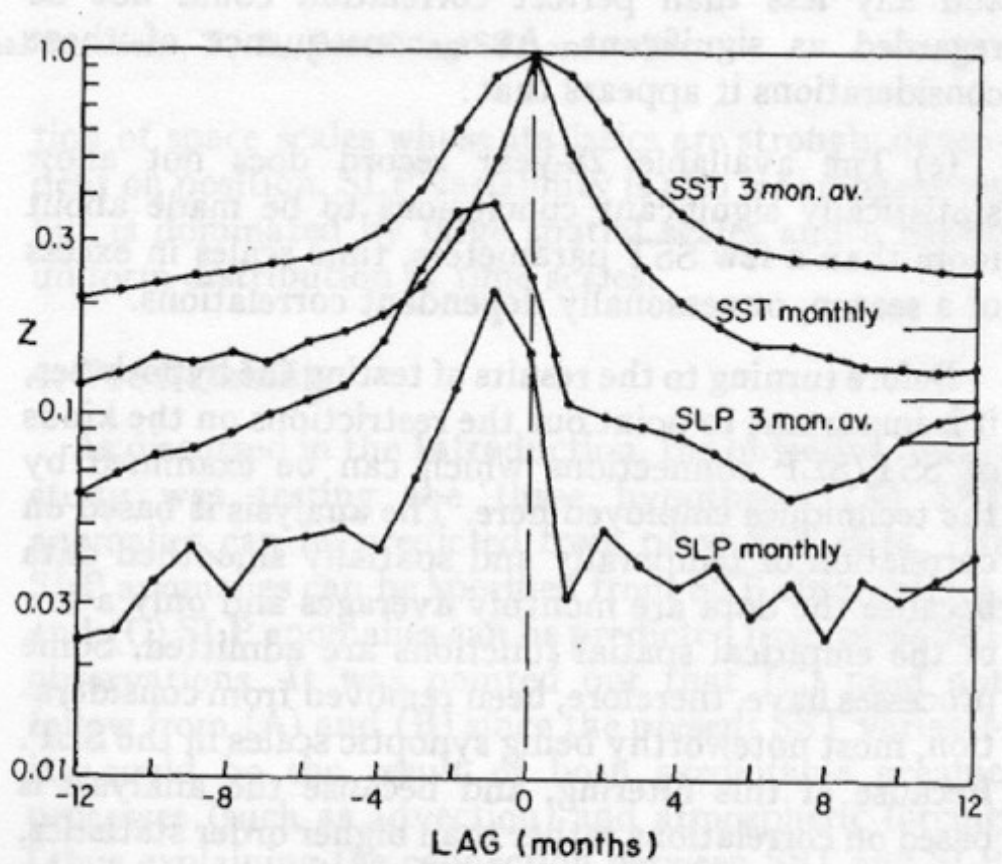

FIG. 7. Skill of estimating SST and SLP in month t+lag using as data ten SST modes from month t. The skill index Z, described in the text, measures the fraction of the entire spatial field correctly estimated. The top two curves refer to estimating one and three month averages of SST; the lower two curves are SLP estimation skill. The horizontal lines at the right are the artificial skill expected when there is no true skill.

Davis 1976

Correlation of SST rate of change (winter) with turbulent heat flux

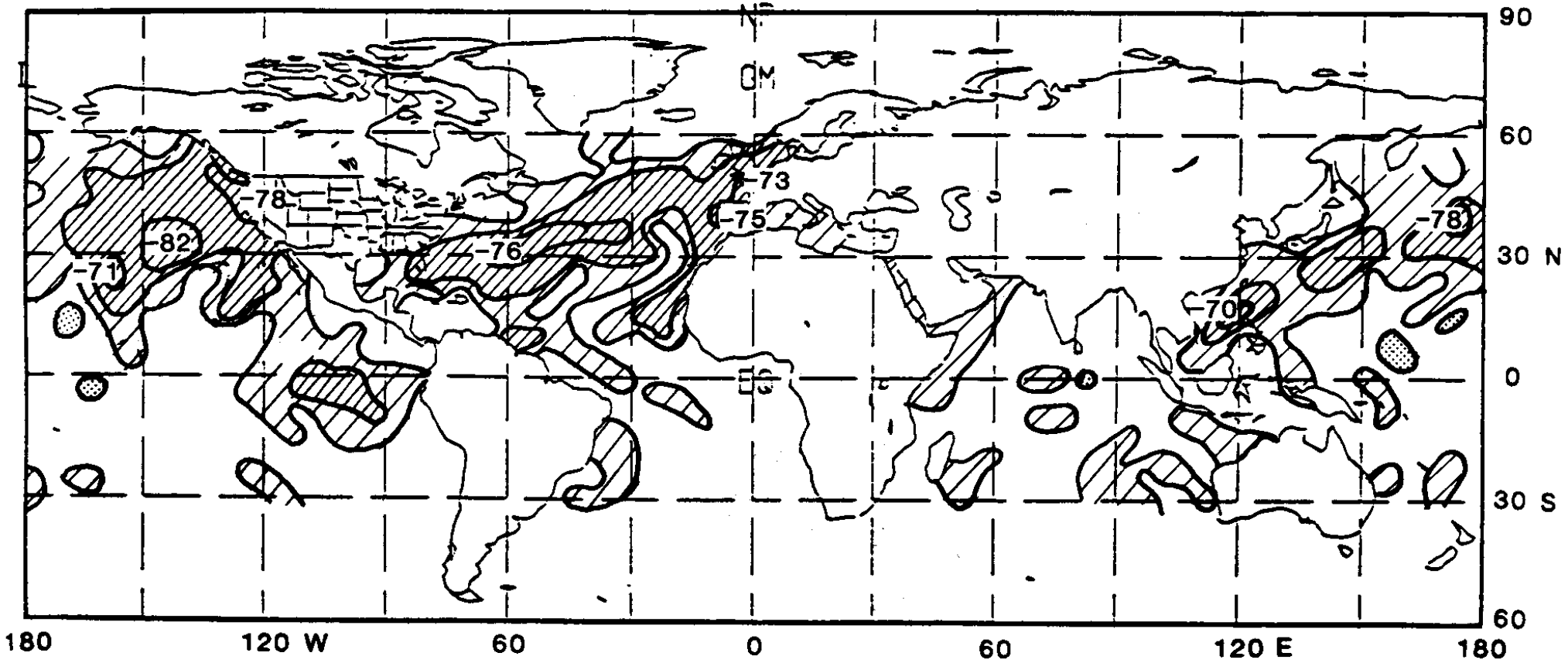

FIG. 2. Correlation coefficients (×100), mapped for global ocean F'_{l+s} vs $\Delta SST'/\Delta t$ at each grid point, for winters 1946–86. Contours at 0, ±0.3, ±0.5, ±0.7. Light and heavy shading indicates correlations ⩽ 0.3 and ⩽0.5. Hatching and stippling denote negative and positive correlations.

ΔSST: 2 month difference within winter

based on COADS data

Cayan 1992

Covariability of anomalies of SST rate of change and turbulent heat flux

CCA between fields

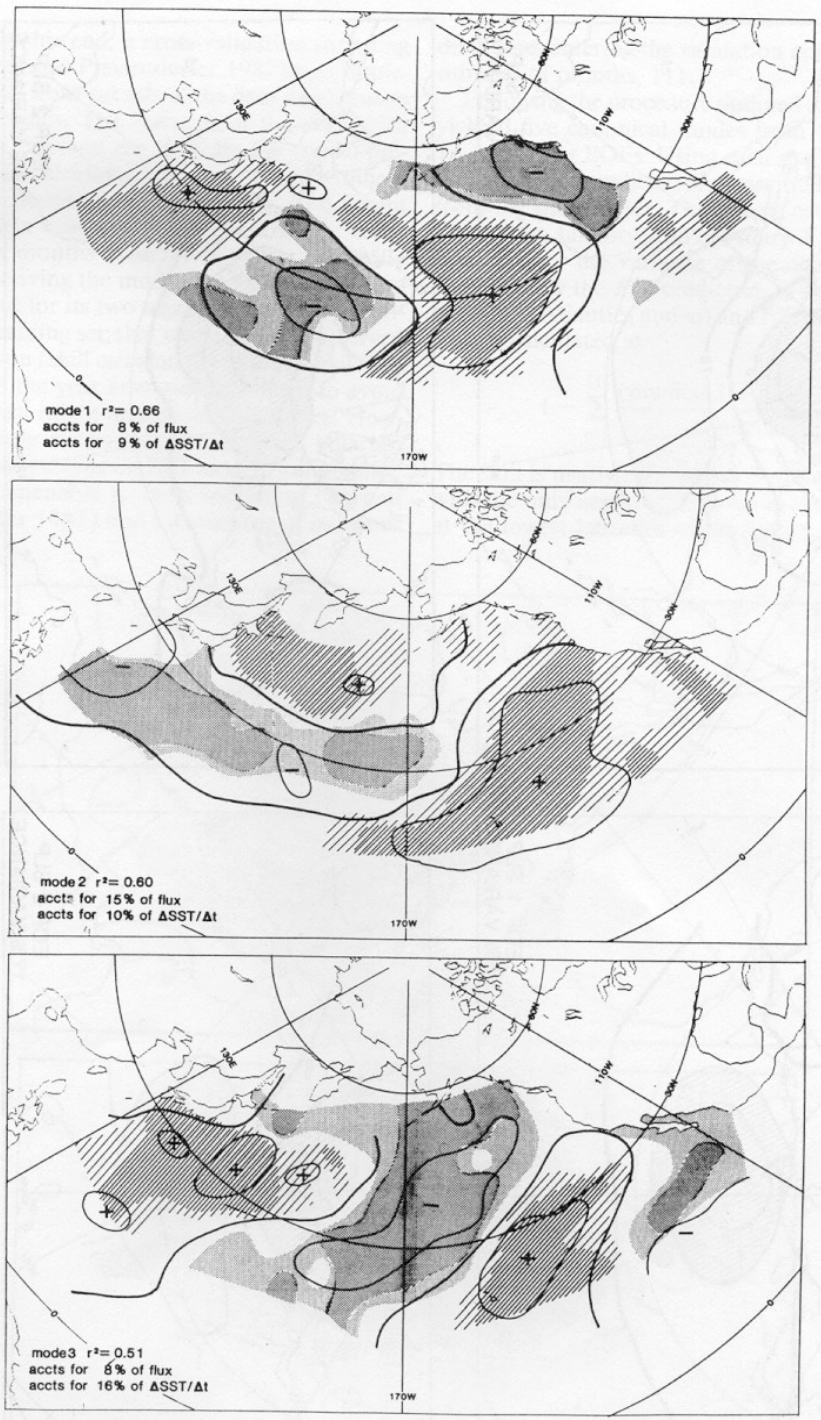

FIG. 4. Spatial patterns for the leading three North Pacific canonical correlation modes: g maps (solid lines), representing F'_{t+s} patterns, vs h maps (shaded), representing $\Delta SST'/\Delta t$ patterns. Contours and shading show relative amplitude of the g and h maps, based on winter months of 1950–86. Positive/negative values of g maps are indicated by +/− signs; positive/negative values of h maps are indicated by stippling/hatching.

Pacific

Cayan 1992

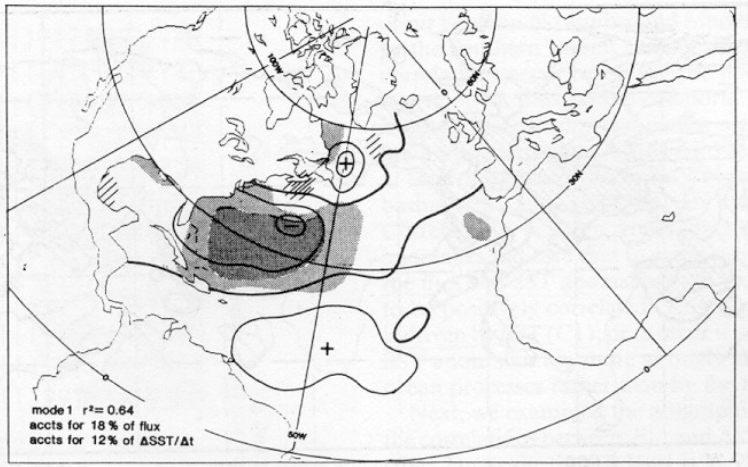

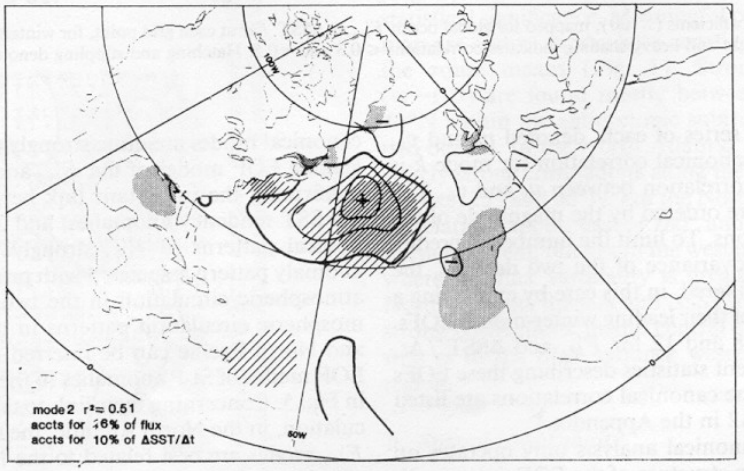

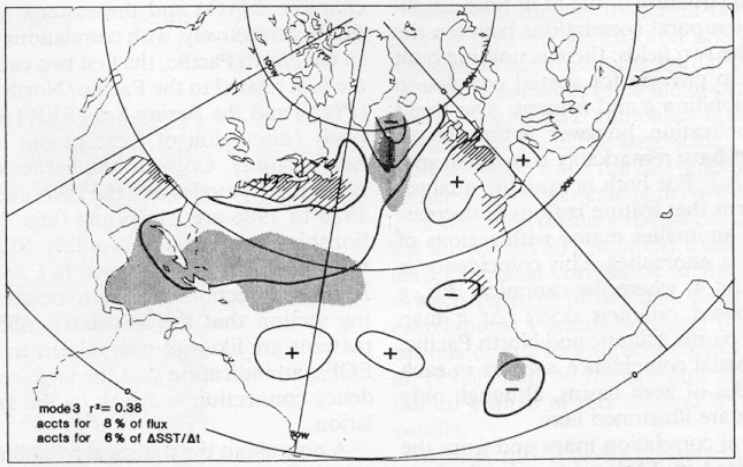

FIG. 3. Spatial patterns for leading three North Atlantic canonical correlation modes: g maps (solid lines), representing F'_{t+s} patterns, vs h maps (shaded), representing $\Delta SST'/\Delta t$ patterns. Contours and shading show relative amplitude of the g and h maps, based on winter months of 1950–86. Positive/negative values of g maps are indicated by $+/-$ signs; positive/negative values of h maps are indicated by stippling/hatching.

Atlantic

Cayan 1992

Surface heat flux and Ekman advection both important

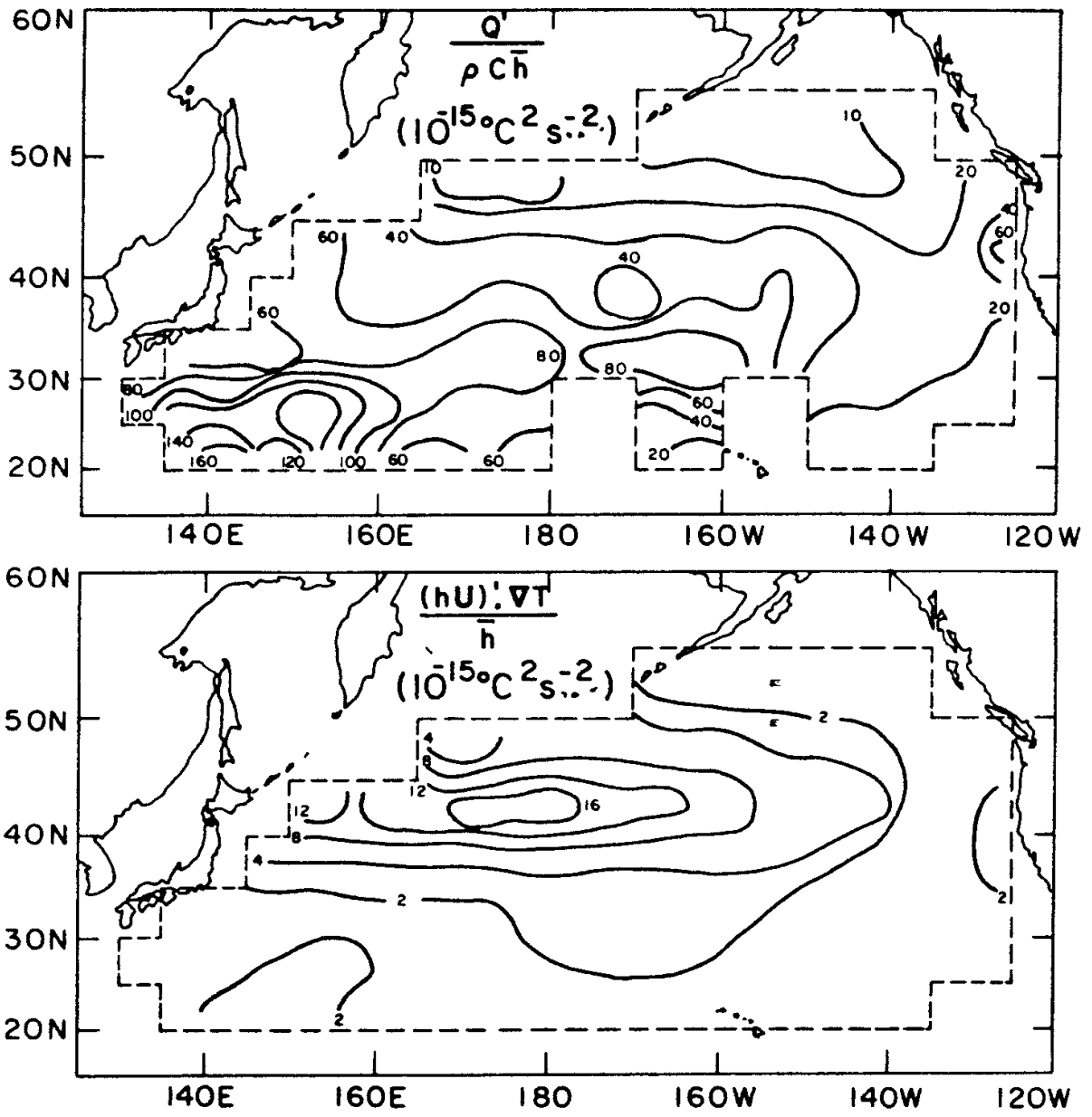

Fig. 7. Variance of monthly anomalies for (top) the heat flux forcing term $Q'/\rho C_p \bar{h}$ and (bottom) the Ekman advection term $-(\tau' \Lambda \mathbf{n}) \cdot \nabla T/\bar{h}$ estimated for the period 1949–1972 [from *Frankignoul and Reynolds*, 1983].

Frankignoul 1985

Linear Response to Heating

Heating acts as a source of vorticity below level of maximum heating (increase of stability), and a sink above the heating (decrease of stability). The vertical integral of the potential vorticity from heating is zero, so heating can not directly force a barotropic response.

Kushnir et al. 2002

Signal to Noise Ratio

Order of anomaly of Z_{500} in response to a surface temperature anomaly T_0' can be estimate from the hypsometric equation

$$Z'_{500} \approx \overline{Z}_{500}\left(\frac{T'_o}{\overline{T}_a} + \frac{1}{ln2}\frac{p'_{surface}}{1000}\right)$$

Baroclinic contribution from first term is 20 m for $T_0' = 1K$.

Barotropic contribution adds about 7m per $p'_{surface} = 1hPA$.

The unforced variations of Z_{500} on monthly to interannual time scales are of the order of 50-100 m. Thus, the forced signal is much smaller than the internal variability, and might be hard to detect.

Does the atmospheric response to SST matter?

Postulated atmospheric response to SST

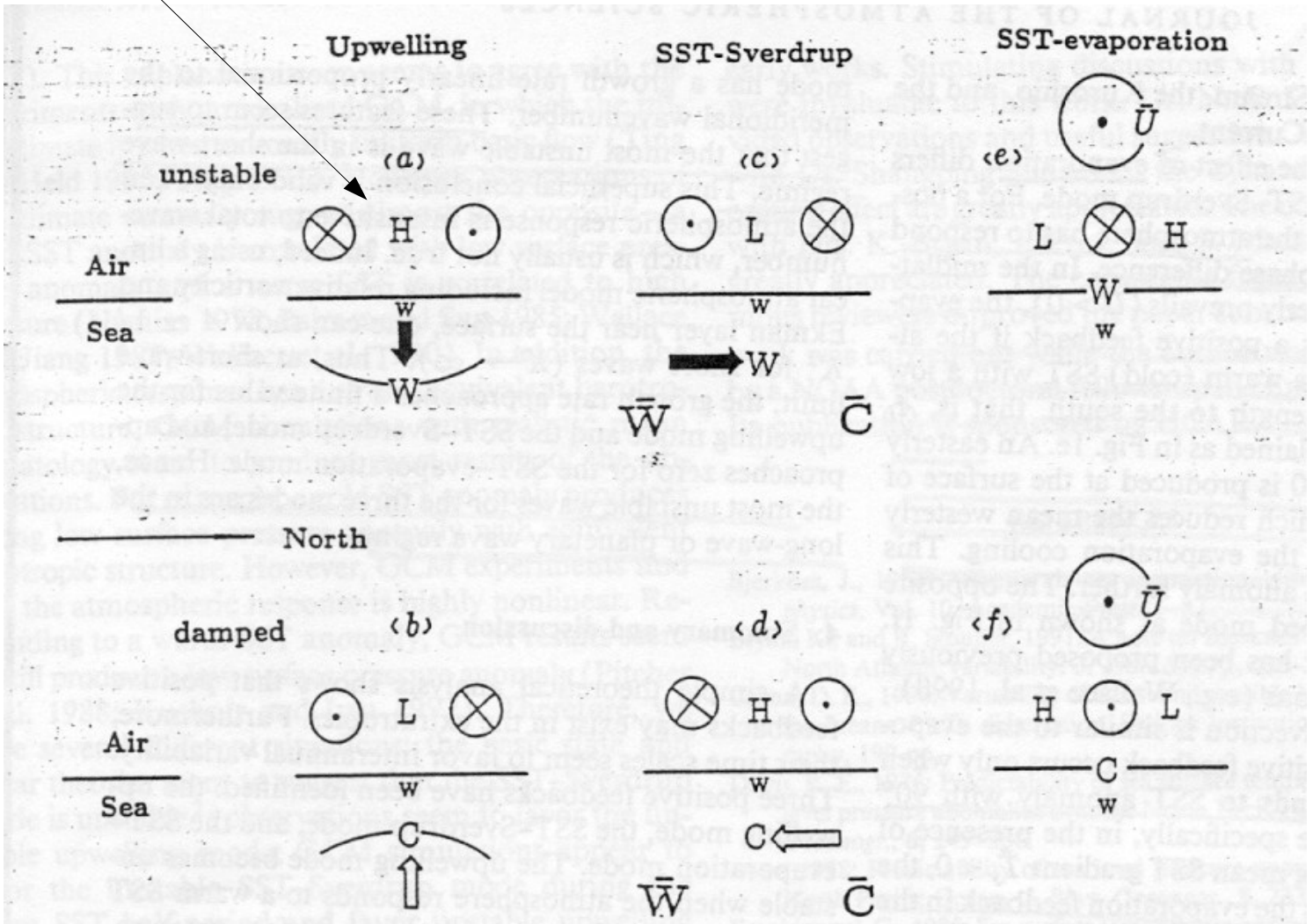

FIG. 1. This schematic figure shows meridional sections of (a) the unstable upwelling mode, (b) damped upwelling mode, (c) unstable SST–Sverdrup mode, (d) the damped SST–Sverdrup mode, (e) the unstable SST–evaporation mode, (f) the damped SST–evaporation mode. In all cases, the initial disturbances are a warm SST anomaly, denoted by a small W; the perturbation temperature due to coupling is denoted by midsized W. The arrows represent current forced by anomalous SST. The $\bar{W}$ and $\bar{C}$ in (c) and (d) represent the mean temperature; $\bar{U}$ is the mean wind. See the text for explanation.

Liu 1993

Scaling of response to thermal forcing (Hoskins and Karoly 1981)

Vorticity and heat budgets linearized about a zonal flow

$$\overline{u}\zeta'_x + \beta v' = fw'_z$$

$$\overline{u}\theta'_x + v'\overline{\theta}_y + w'\overline{\theta}_z = \frac{\theta_0}{g}Q$$

This yields

$$f\overline{u}v'_z - f\overline{u}_z v' + w'N^2 = Q$$

if zonal advection dominates

$$v' \sim \frac{QH_Q}{f\overline{u}}$$

if meridional advection dominates

$$v' \sim \frac{QH_U}{f\overline{u}}$$

if vertical advection dominates (use heat budget and vorticity balance between vortex stretching and advection of planetary vorticity

$$v' \sim \frac{fQ}{\beta N^2 H_Q}$$

where the vertical scales are

$$H_Q = \frac{Q}{Q_z}$$

$$H_U = \frac{\overline{u}}{\overline{u}_z}$$

$$H = min(H_Q, H_U)$$

Comparing horizontal to vertical advection

$$\gamma = \frac{f^2\overline{u}}{\beta N^2 H_Q H}$$

shows that heatig is balanced by vertical advection for $\gamma << 1$ and by horizontal advection for $\gamma >> 1$.

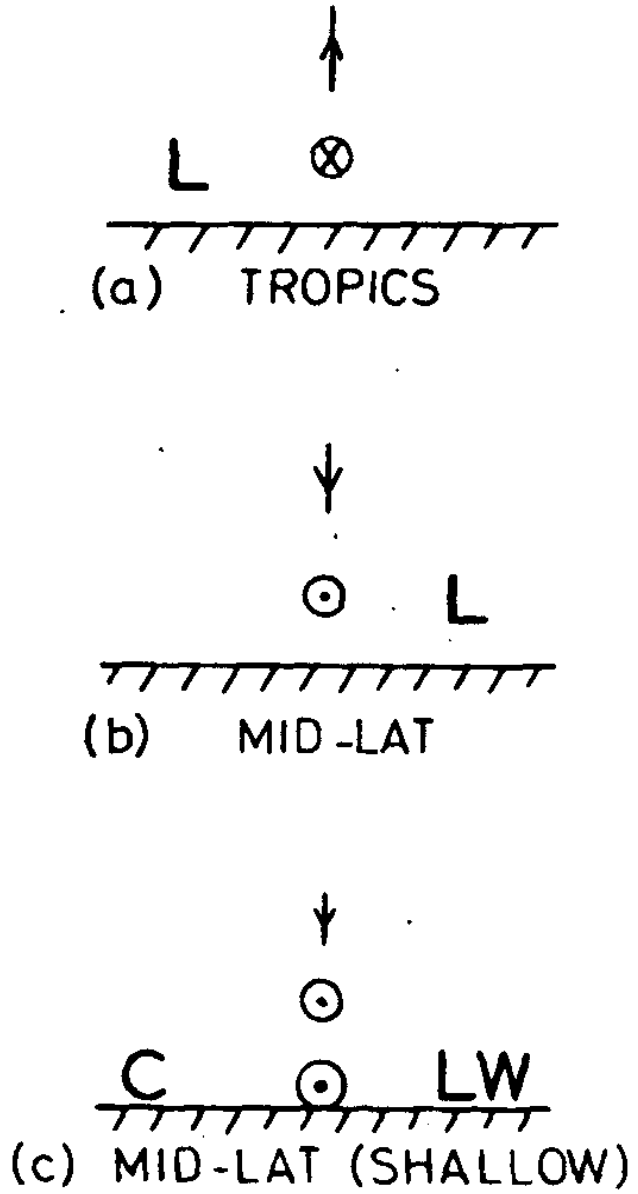

FIG. 2. Longitude-height sections showing the differing responses to thermal forcing in (a) tropics, (b) midlatitudes, and (c) mid-latitudes for shallow forcing. The arrow depicts vertical motion, circled crosses and dots motion into and out of the section, respectively, L the pressure trough, and C and W cold and warm air, respectively.

shallow heating leads to very large v'

if deep heating H_Q > 1 km then $\gamma << 1$

Q>0 away from surface implies w'>0, dw/dz>0, v'>0 and trough to the west

γ typically large, heating is balanced by horiz. advection

$H_Q > H_U$, heat source is balance by advection from pole: v'<0, the trough is to east, dw/dz<0 and downward motion

shallow heating: zonal advection, i.e. have to have a temperature gradient in zonal direction, trough in east and cool air advection from pole

Hoskins and Karoly 1981

Response of a linear, QG model to impose heating

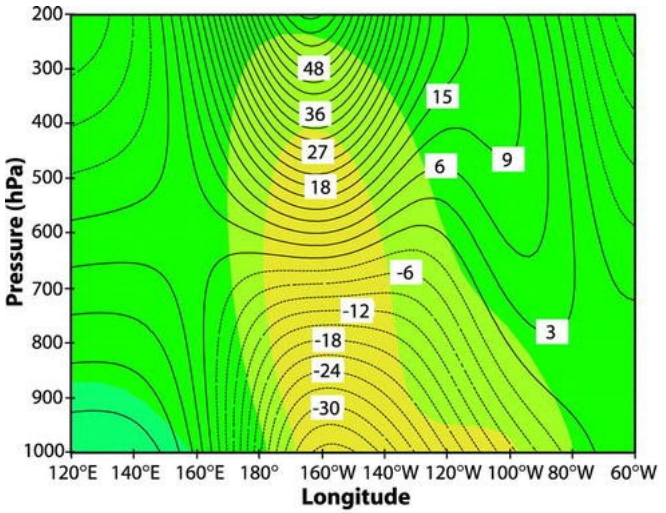

Deep heating

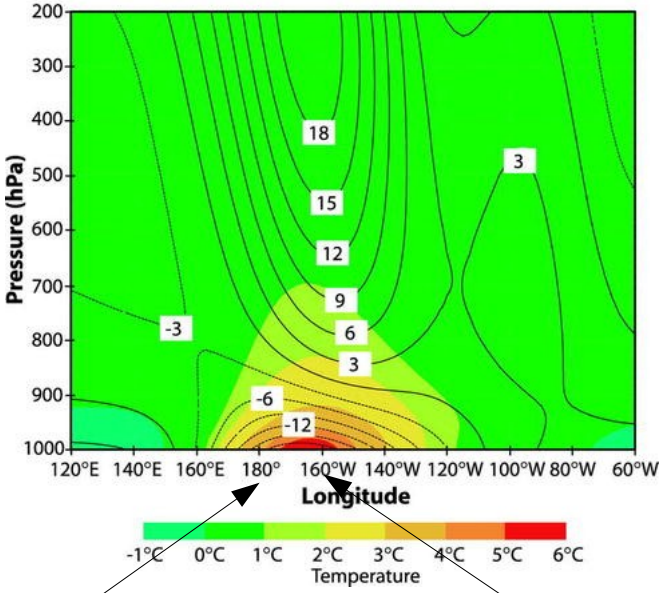

Shallow heating

Heating location

Surface low

Kushnir et al. 2002

Does the response of the atmosphere matter II?

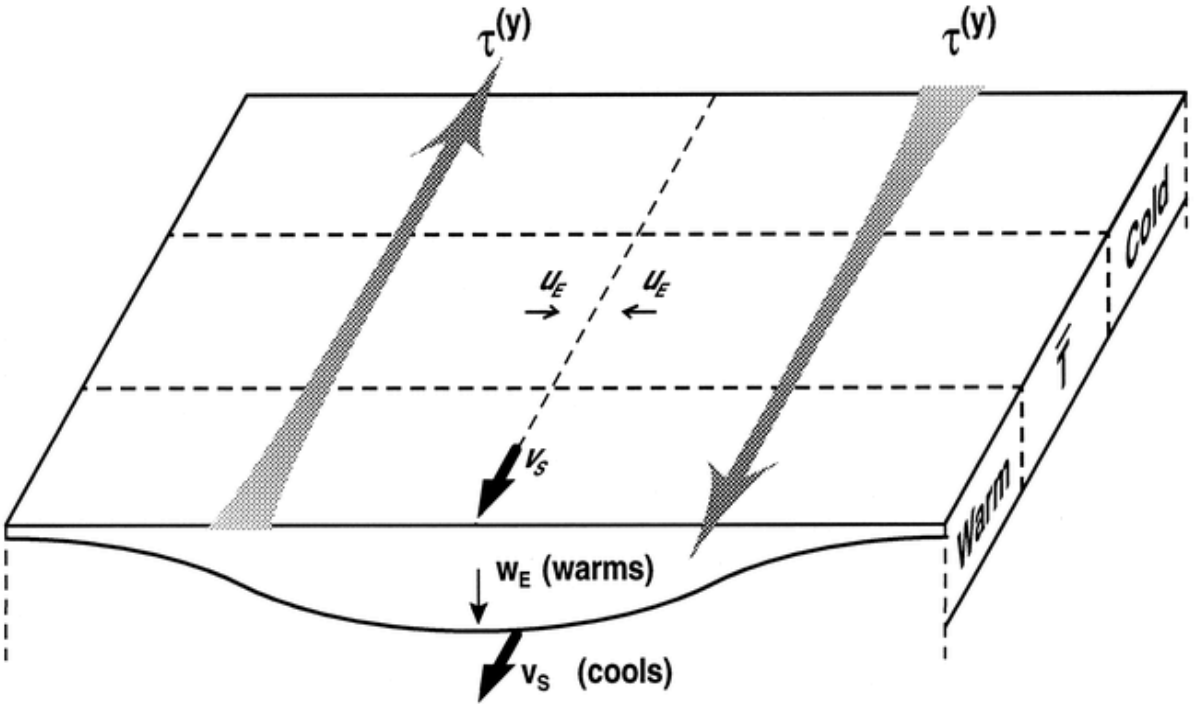

Consider simple single layer ocean, with SST being affected by Ekman advection, Sverdrup flow, vertical advection, similar to what we used in the tropics.

Talley 1999

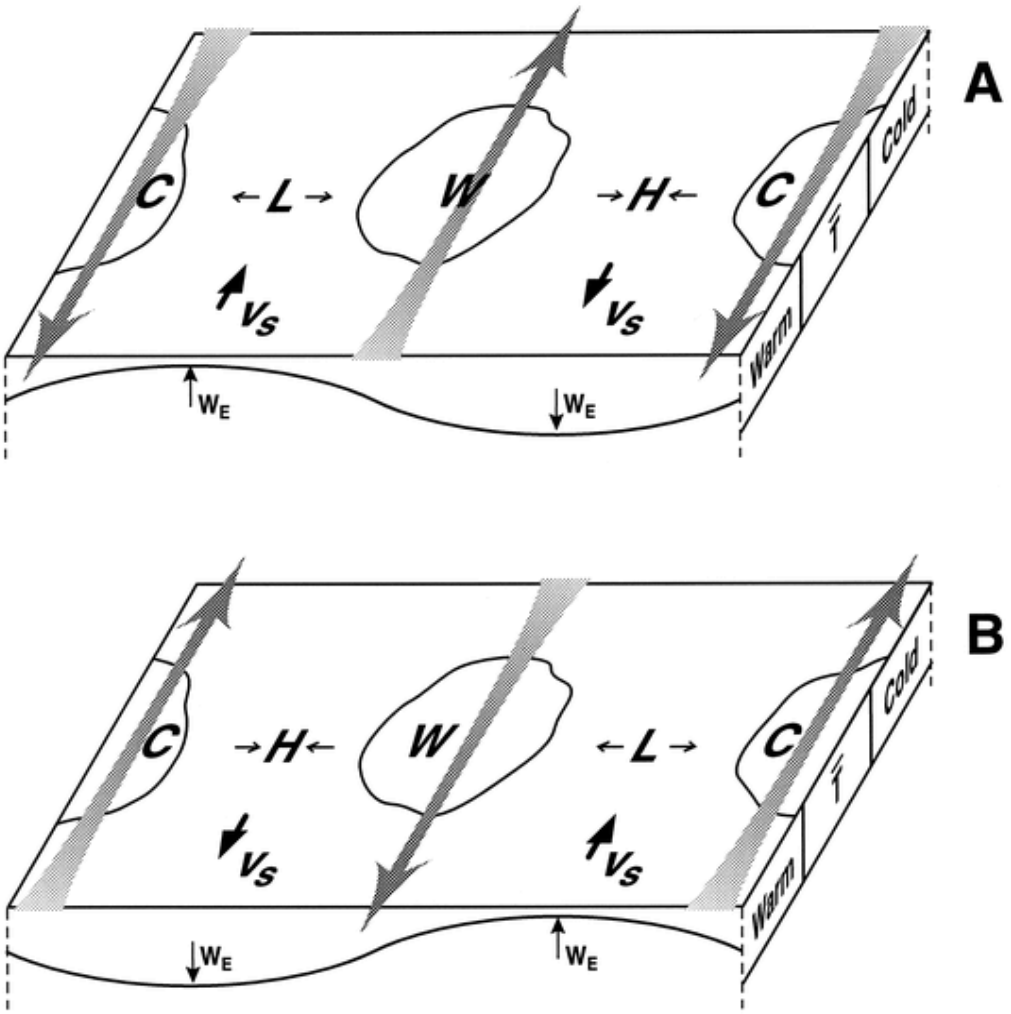

Atmosphere, heating colocated with SST

vertical advection balances heating

Zonal advection balances heating

Depending on atmospheric response and ocean heat flux anomalies can propagate east- or westward, at different speeds.

Talley 1999

Ocean	Atmosphere			
	Vertical advection $w\ (\partial\overline{\theta}/\partial z) = Q_A$	Zonal advection $u_A\ (\partial\theta/\partial x) = Q_A$	Zonal advection, assuming equivalent barotropic $u_A\ (\partial\theta/\partial x) = Q_A$	Temperature relaxation $0 = Q_A - r\theta$
Ekman pumping $\partial T'/\partial t + \overline{u}(\partial T'/\partial x) = -\gamma w_E$	SLP high downstream of SST high Baroclinic atmosphere Eastward propagation relative to mean ocean flow	SLP low downstream of SST high Baroclinic atmosphere Westward propagation relative to mean ocean flow	SLP high downstream of SST high Equivalent BT atmosphere Eastward propagation relative to mean ocean flow	SLP low over SST high Baroclinic atmosphere Advected with the mean ocean flow Damped due to atmosphere relaxation
Surface heat flux $\partial T'/\partial t + \overline{u}(\partial T'/\partial x) = -\kappa T'$	SLP high downstream of SST high Baroclinic atmosphere Advected with the mean ocean flow Damped due to ocean	SLP low downstream of SST high Baroclinic atmosphere Advected with the mean ocean flow Damped due to ocean	SLP high downstream of SST high Equivalent BT atmosphere Advected with the mean ocean flow Damped due to ocean	SLP low over SST high Baroclinic atmosphere Advected with the mean ocean flow Damped due to ocean
Sverdrup response and surface heat flux $\partial T'/\partial t + \overline{u}(\partial T'/\partial x) = -v_S(d\tilde{T}/dy) - \kappa T'$	SLP high downstream of SST high Baroclinic atmosphere Westward propagation relative to mean ocean flow Damped due to ocean	SLP low downstream of SST high Baroclinic atmosphere Eastward propagation relative to mean ocean flow Damped due to ocean	SLP high downstream of SST high Equivalent BT atmosphere Westward propagation relative to mean ocean flow Damped due to ocean	SLP low over SST high Baroclinic atmosphere Advected with the mean ocean flow Damped due to ocean Growth due to atmosphere relaxation

Talley 1999

Atmosphere

Model	Phase speed	Phase speed (cm s^{-1})
Vertical advection; Ekman response	$u_{ev} = G_1 \frac{\gamma\lambda}{\rho_o \delta \beta}$	4
Vertical advection; Sverdrup response	$u_{Sv} = G_1 \frac{f}{\beta^2} \frac{\lambda}{\rho_o \delta h_S} \frac{d\overline{T}}{dy}$	−18
Zonal advection, rigid-lid; Ekman response	$u_{ez} = -G_2 \frac{\gamma}{\rho_o \delta} \frac{\lambda}{f^2 \overline{u}_A}$	−1
Zonal advection, rigid-lid; Sverdrup response	$u_{sz} = -G_2 \frac{\lambda}{f \overline{u}_A} \frac{1}{\rho_o \delta \beta h_S} \frac{d\overline{T}}{dy}$	5
Zonal advection, equivalent barotropic; Ekman response	$u_{ezbt} = \frac{\gamma \epsilon_1}{\rho_o \delta f^2 \overline{u}_A}$	2
Zonal advection, equivalent barotropic; Sverdrup response	$u_{szbt} = \frac{\epsilon_1}{\rho_o f \overline{u}_A \beta \delta h_S} \frac{d\overline{T}}{dy}$	−10
	Decay rate	Decay rate (s^{-1})
Atmosphere relaxation; Ekman response; damping	$\kappa + k^2 G_3$	6×10^{-8} (10 000 km wavelength)
Atmosphere relaxation; Sverdrup response; damping	$\kappa - k^2 G_4$	-1×10^{-7} (10 000 km wavelength)

Ocean

Talley 1999

Statistical estimation of the atmospheric response

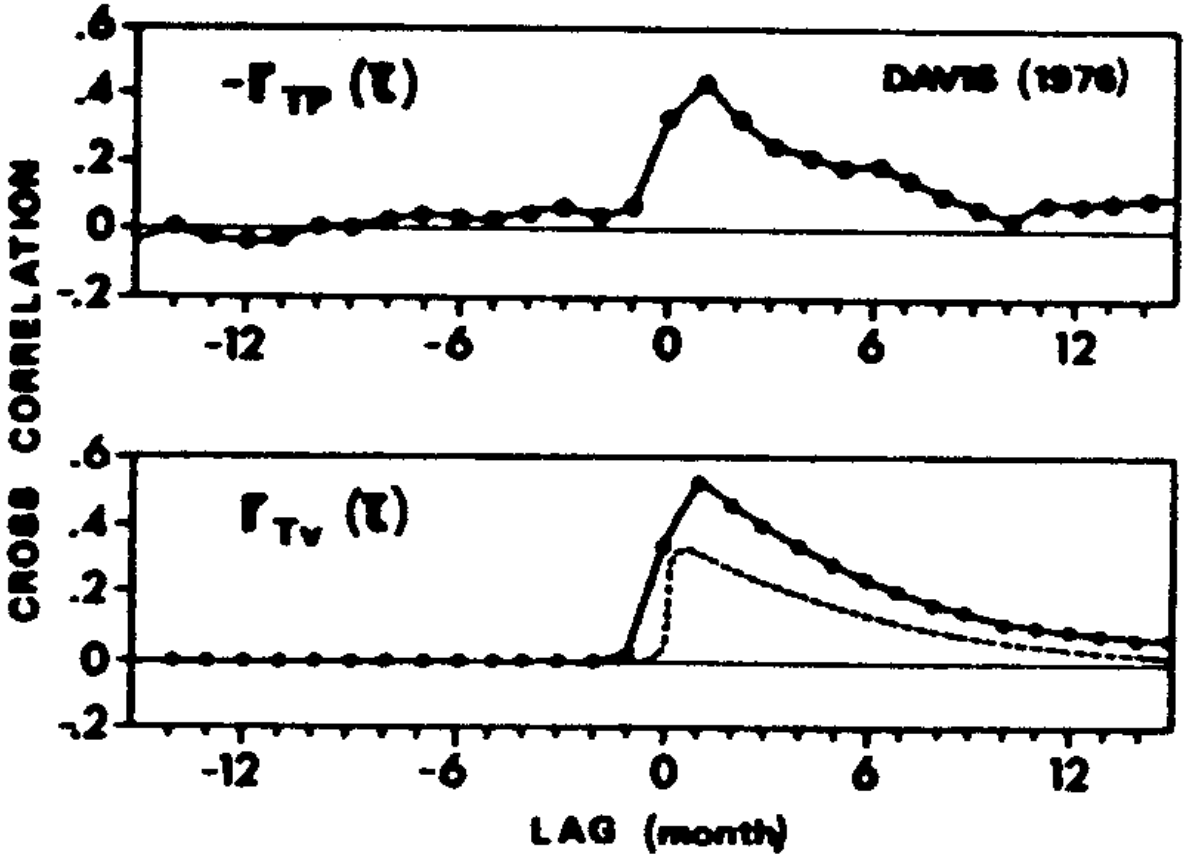

Fig. 20. (Top) Observed correlation between the dominant empirical orthogonal function of SST and sea level pressure anomalies over the North Pacific as estimated by *Davis* [1976]. (Bottom) Theoretical correlation for $\nu = (8.5 \text{ day})^{-1}$, $\lambda = (6 \text{ month})^{-1}$ without smoothing (dashed line) and as estimated from monthly averaged data (continuous line).

Frankignoul 1985

But this is not all: Correlation of leading SSTs and SLP in North Atlantic

Reemergence

SST leading SLP

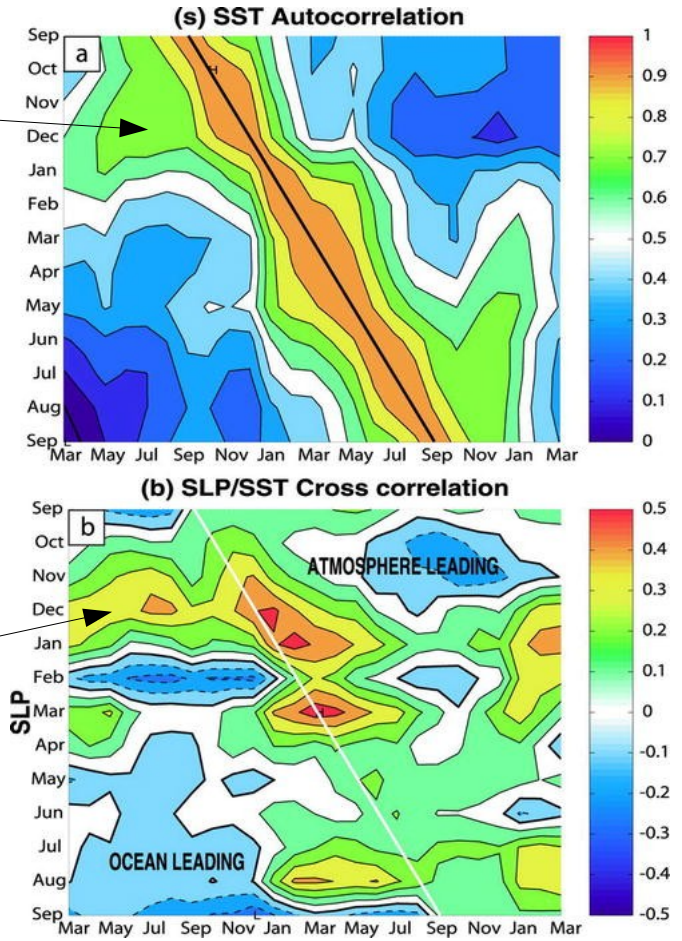

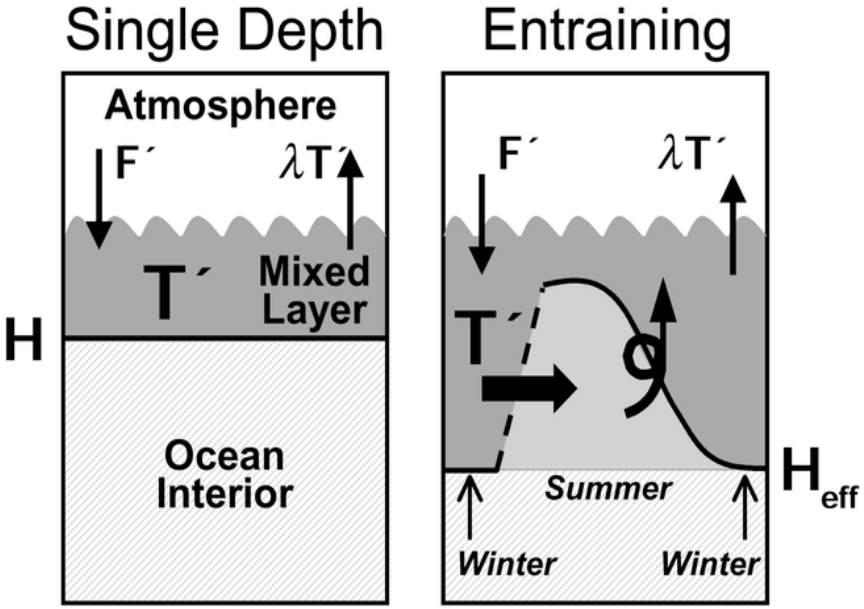

Kushnir et al. 2002

SVD between winter time Z500 and lagged SST

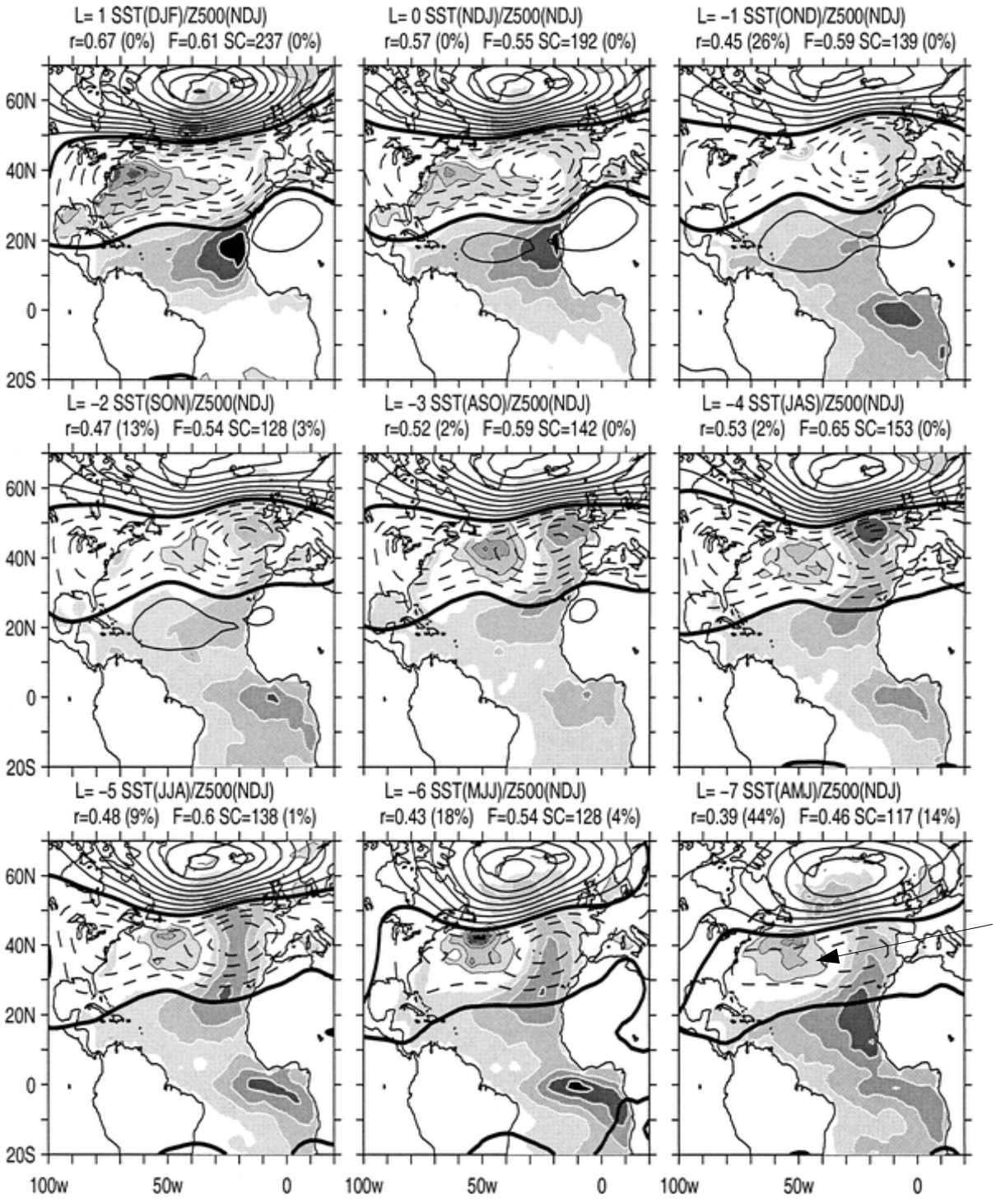

SST leading by 6 month

Czaja and Frankignoul 2002

How can a barotropic response be generated?

Transient eddy response: eddy export of vorticity aloft is balanced by mean convergence, mid level descent, and low level mass divergence, leading to vortex shrinking close to the surface and a low.

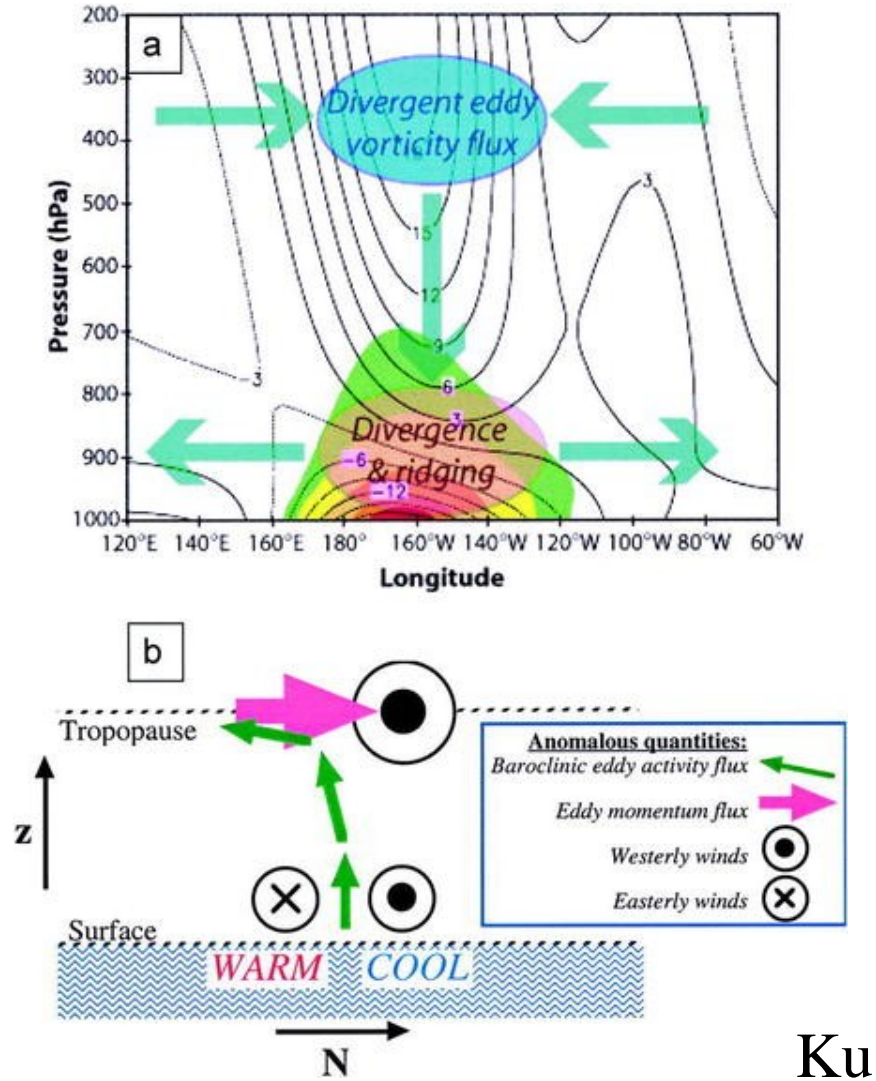

Kushnir et al. 2002

What do AGCM experiment with prescribed SST anomalies tell us?

-atmosphere responds, with 10-20gpm/K at Z500

-surface fluxes tend to dampen SST anomalies at 10-20W/m^2K

-precipitation anomalies occur close to SST anomalies, diabatic heating is shallow compared to tropics

-temperature in lower troposphere mirrors SST, decays rapidly with height

-the response is very sensitive to model's climatological state and storm track

Sensitivity of atmospheric response to SST anomalies

Reference	SST anomaly (location and size)	Model resolution	Experimental design	Response pattern
Palmer and Sun (1985)	Western North Atlantic; 3 K	Grid point ~ 330 km with 5 levels	5 sets of 50-day runs with positive and negative SSTA, each starting with different November initial conditions	EqBt high downstream of positive SSTA; 20 m K^{-1} at 500 hPa; 1.5 hPa K^{-1} at SLP
Pitcher et al. (1988)	North Pacific; 2 and 4 K	Spectral R15 with 9 levels	Perpetual Jan; 1200-day runs with positive and negative SSTA, compared to similar control run	EqBt low downstream of both positive and negative SSTA; 25 m K^{-1} at 500 hPa; 1.2 hPa K^{-1} at SLP
Kushnir and Lau (1992)	North Pacific; 2 K (similar to Pitcher et al.)	Spectral R15 with 9 levels	Perpetual Jan; positive and negative SSTA and control each for 1350-days and 9 sets of 180-day transient runs	EqBt low downstream of both positive and negative SSTA; slow transient adjustment; 20 m K^{-1} or 2 hPa K^{-1}
Ferranti et al. (1994)	Western North Pacific and North Atlantic; 2 K	Spectral T63 with 19 levels	5 pairs (positive and negative SSTA) of 120-day runs starting with Nov initial conditions and continuing to Feb	Only 500 hPa shown; high (low) downstream of positive (negative) SSTA; 20 m K^{-1}
Peng et al. (1995)	Western North Atlantic; 3 K	Spectral T42 with 21 levels	50-day positive and negative SSTA and control runs for 6 perpetual Nov and 4 perpetual Jan cases	Downstream of positive SSTA EqBt high in Nov, but EqBt low in Jan; 30–40 m K^{-1} or 3 hPa K^{-1}
Kushnir and Held (1996)	Central North Atlantic; 4 K	Spectral R15 with 9 levels	6000-day perpetual Jan and Oct runs with positive and negative SSTA; parallel runs with idealized GCM	All runs show weak baroclinic response with surface low and upper level high downstream of positive SSTA
Latif and Barnett (1995, 1996)	North Pacific basin; 1 K	Spectral T42 with 19 levels	18-month runs with perpetual Jan conditions, positive and negative SSTA	Positive–negative composite has strong EqBt high downstream of positive SSTA; 5 hPa K^{-1} at SLP
Peng et al. (1997)	Central North Pacific; 2.5 K	Spectral T40 with 18 levels	Two cases (perpetual Jan and Feb) each has 4 pairs (positive SSTA and control) of 96-month run	Downstream of positive SSTA EqBt high (10 m K^{-1}) in Feb but baroclinic low (1 hPa K^{-1}) in Jan

Note the differences in baroclinic/barotropic nature and of the linearity of response. This suggests the importance of background state, baroclinic eddy feedback, and the interaction with the intrinsic variations at the atmosphere.

Kushnir et al. 2002

Source of non-linearity

- stationary nonlinear forcing, usually not that important

- transient eddy forcing

- nonlinearities of physical parameterizations (surface fluxes)

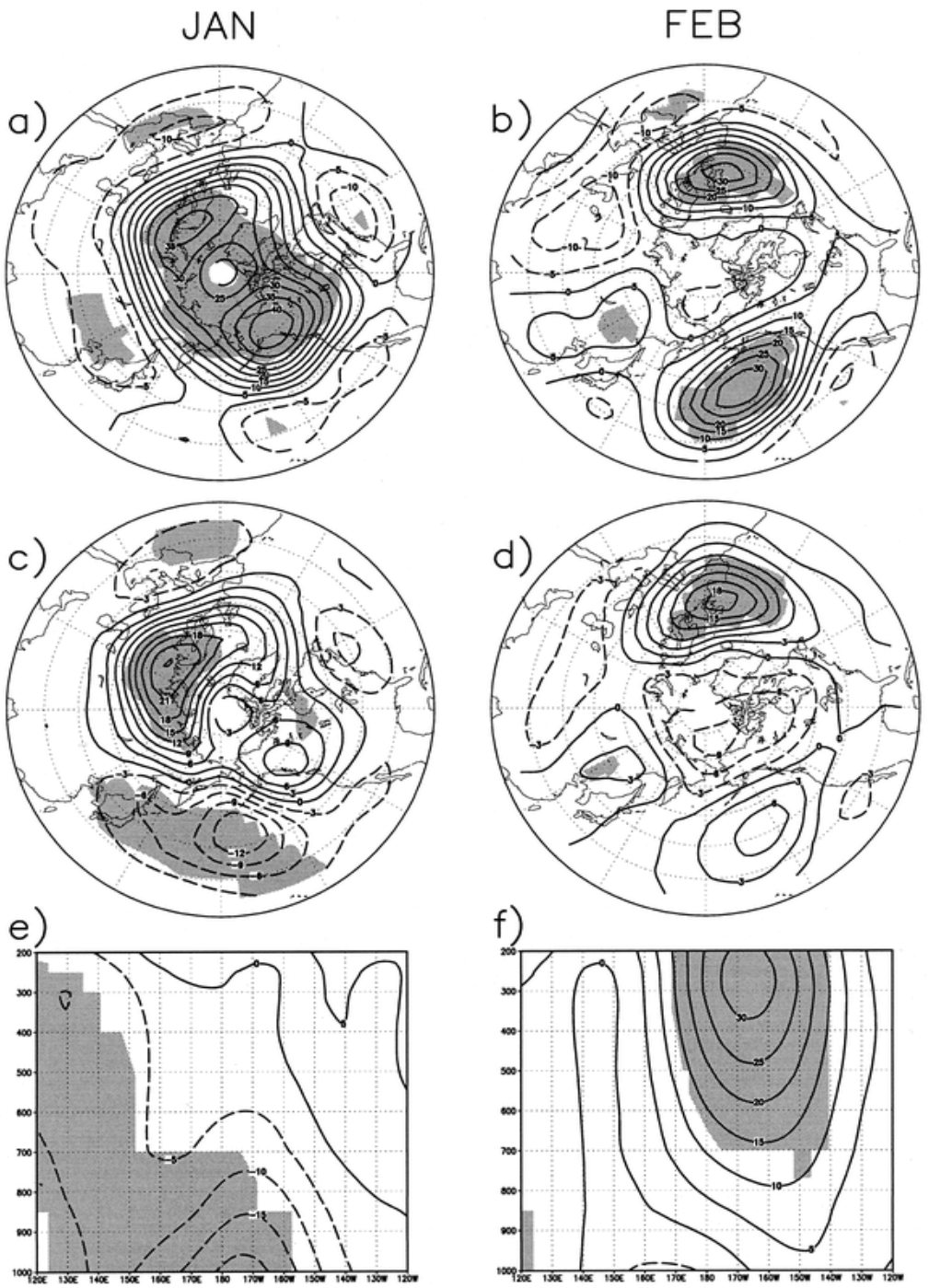

AGCM response to SST anomaly in the western North Pacific for January and February mean conditions.

Peng and Whitacker 1999

Sensitivity to background state

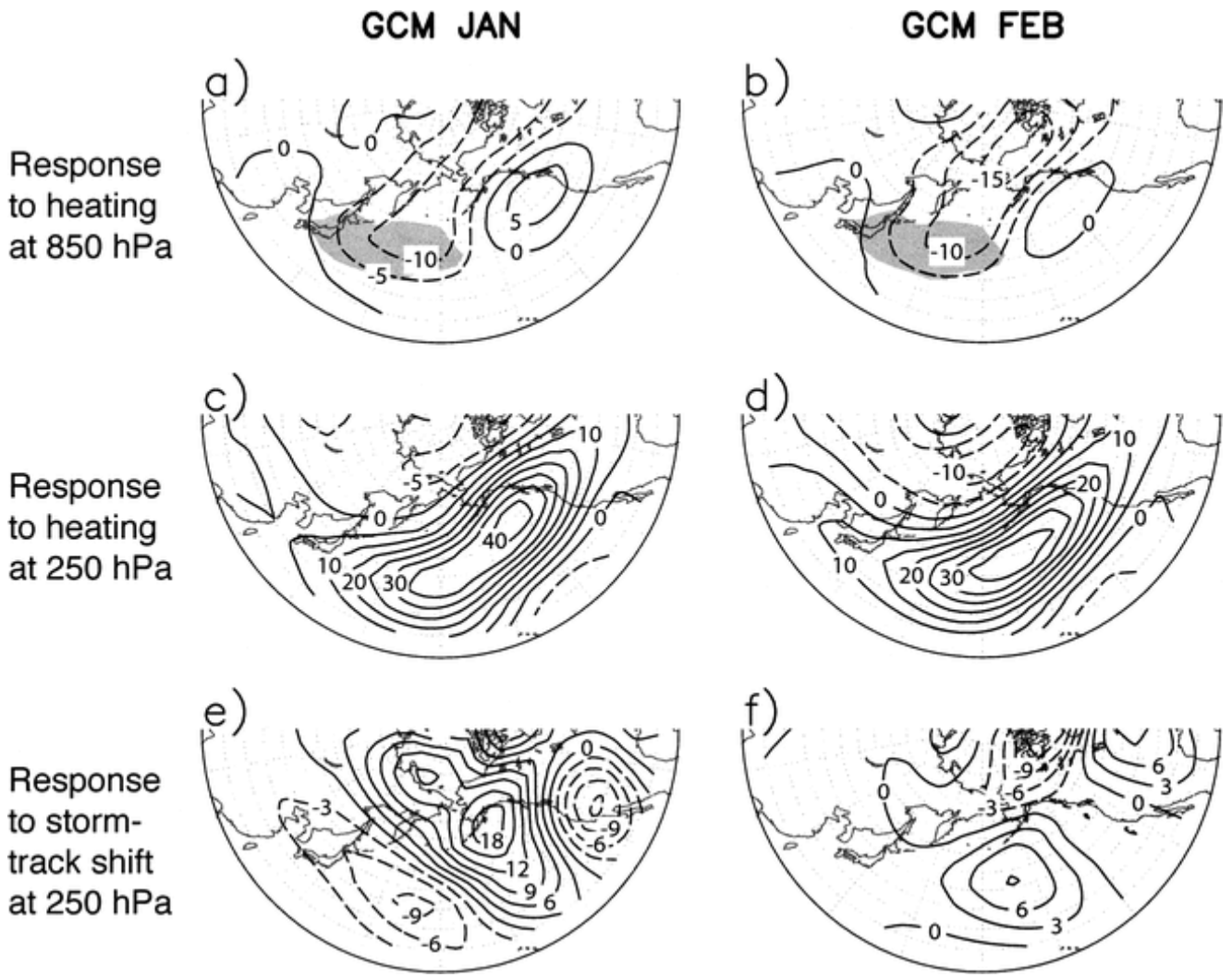

Linear response to NP SST anomaly

Response to heating anomaly predicted by storm track model

Kushnir et al. 2002

Potential Predictability:
How much of the variance of SLP is due to SST anomalies?

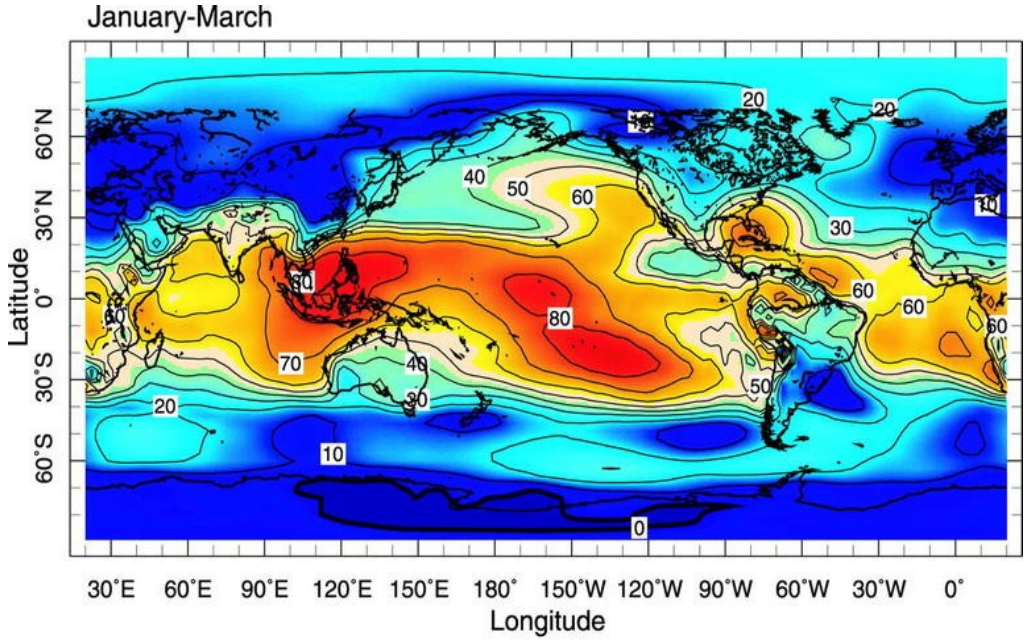

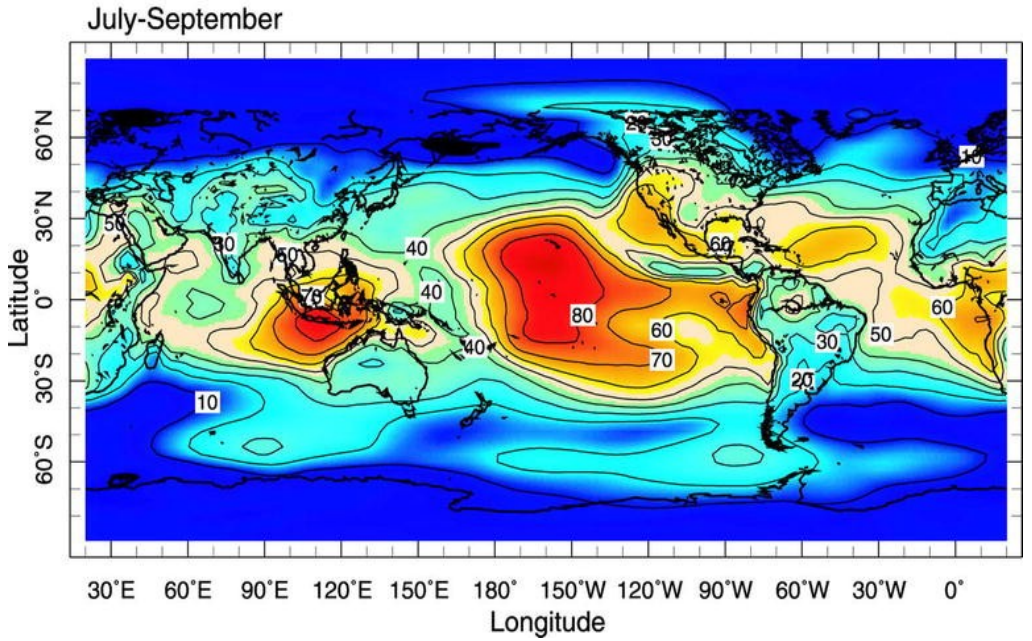

Ratio of variance ensemble mean and total SLP

Note the striking difference between the tropics and extra-tropics.

Kushnir et al. 2002

Problems with AMIP type experiments

Reanalysis

AGCM ensemble avg.

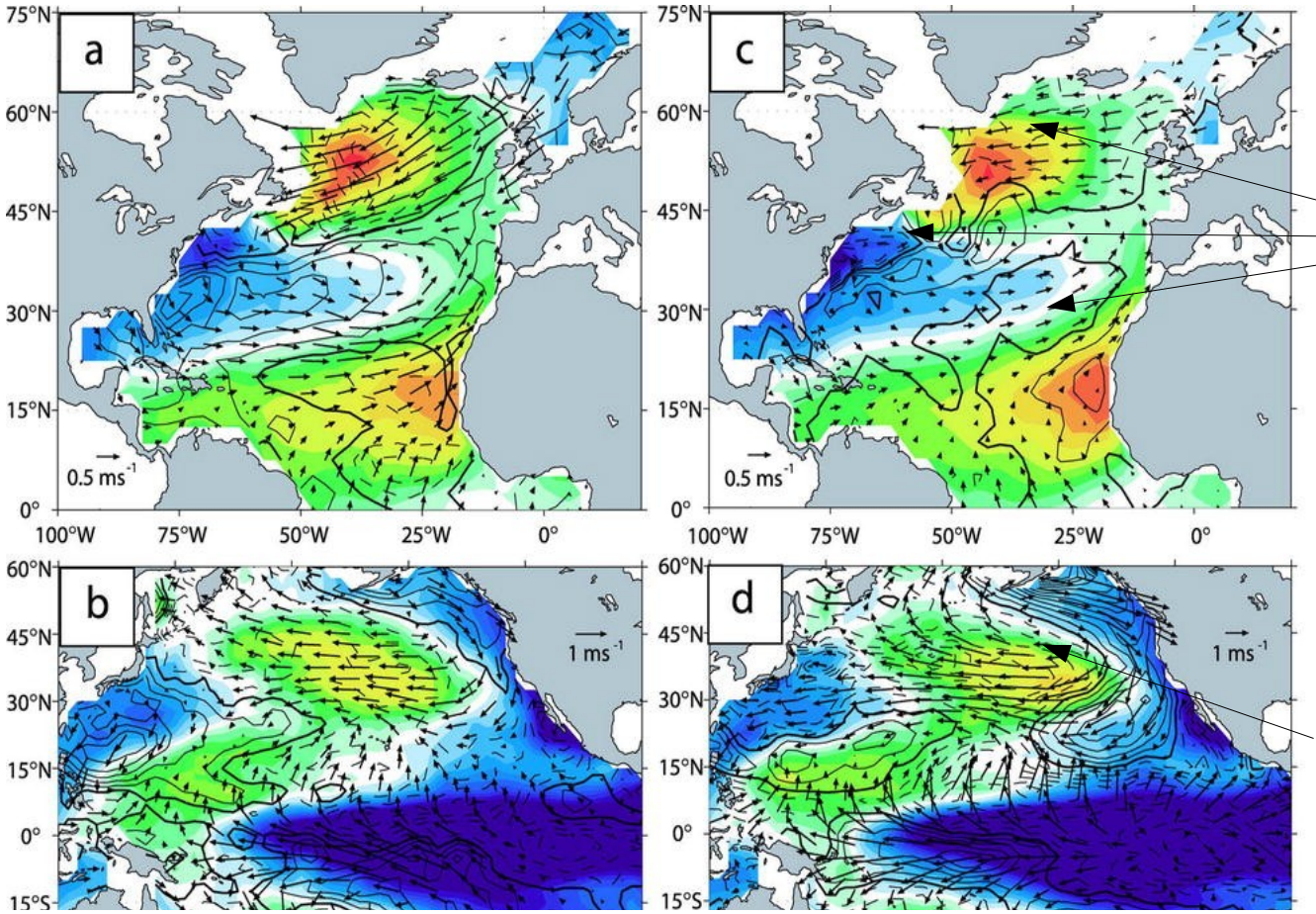

Weak response

Teleconnected tropical forcing

Reduce amplitude response in AMIP ensemble can reflect the unrealistic imprint of the prescribed, single realization of SST on the atmosphere, even though no feedback existed originally (Bretherton and Battisit 2000).

Windows to the ocean's circulation

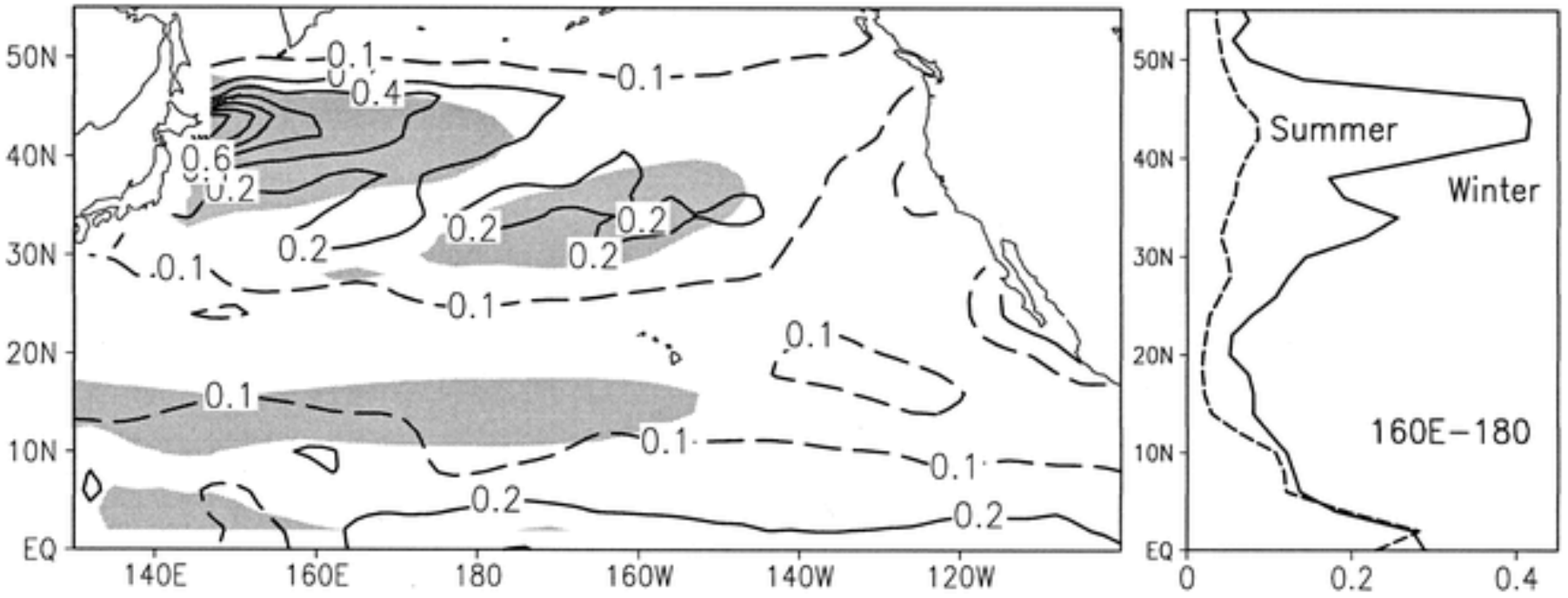

STD of SST (contours) and temperature at 200 m simulated by OGCM (>0.3C/0.6C N/S of 20N) forced by anomlous wind stress only, SST and SSS are relaxed to climatology. Note that only special areas (KOE in winter) act as a window of the surface layer to thermocline anomalies.

Xie et al. 1999

Air-Sea Interaction

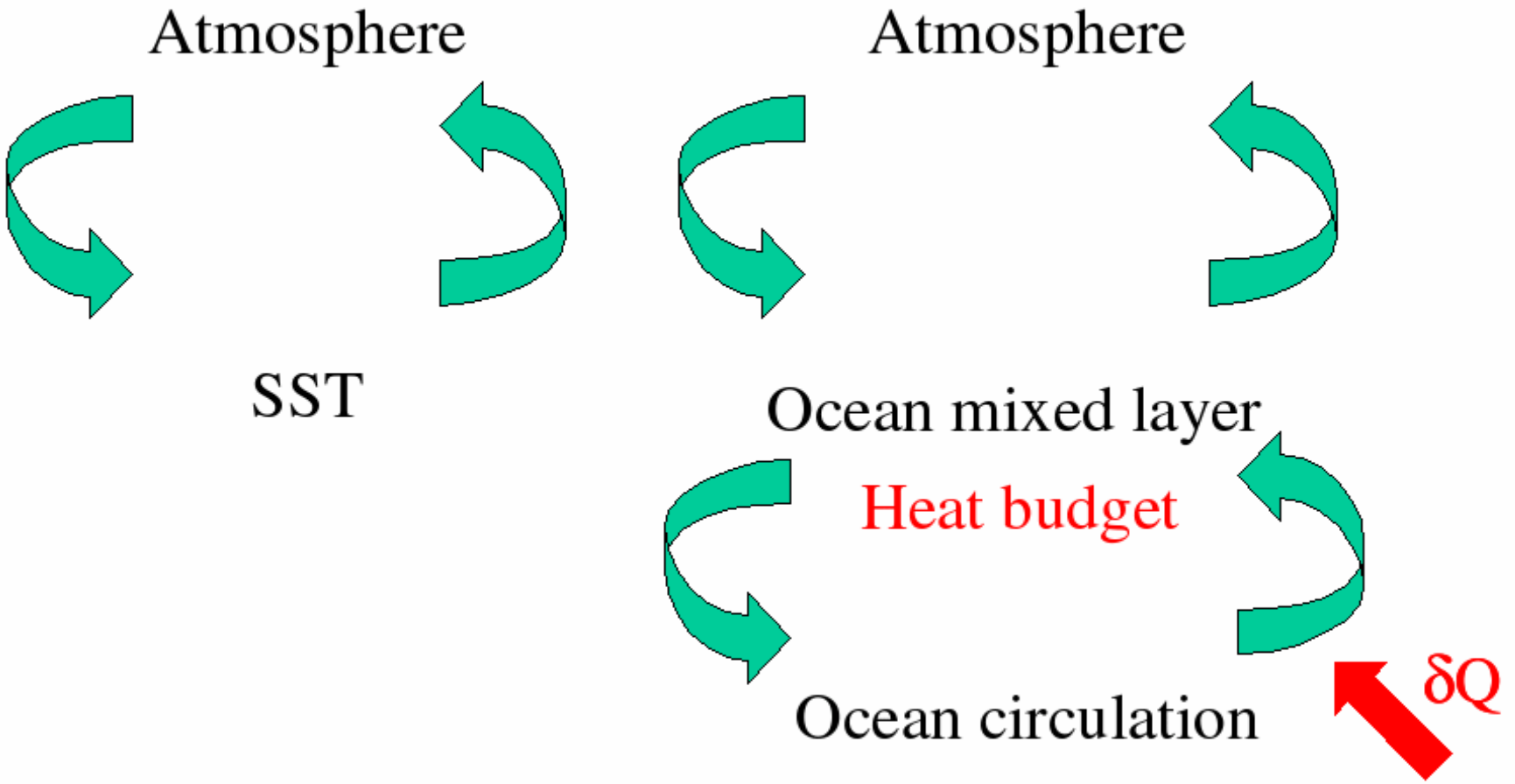

Yulaeva et al. (2001)

Sutton and Mathieu (2002)

Prescibe oceanic heat flux convergences in a AGCM coupled to a slab ocean (mixed-layer ocean).

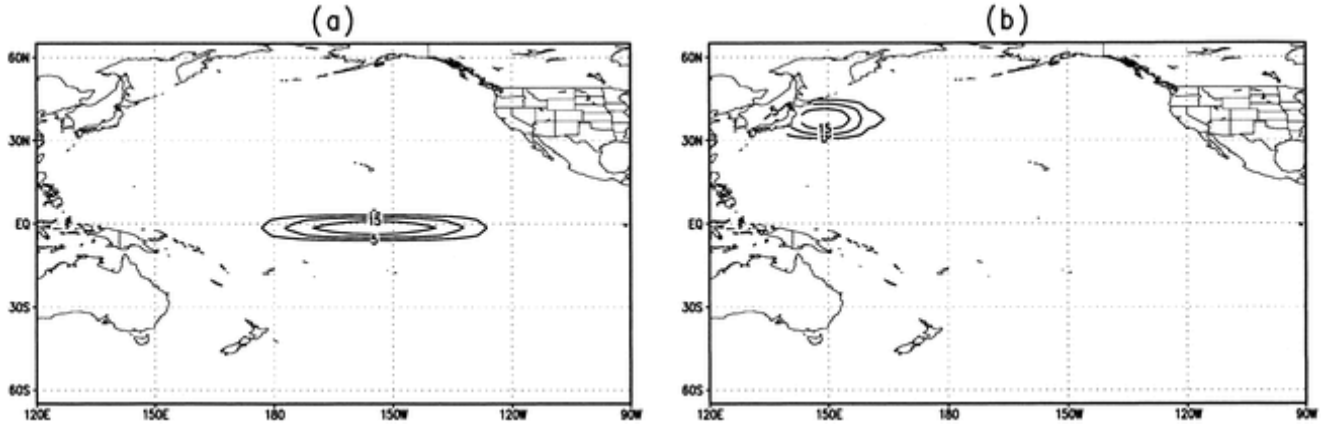

Yulaeva et al. 2000

Latent

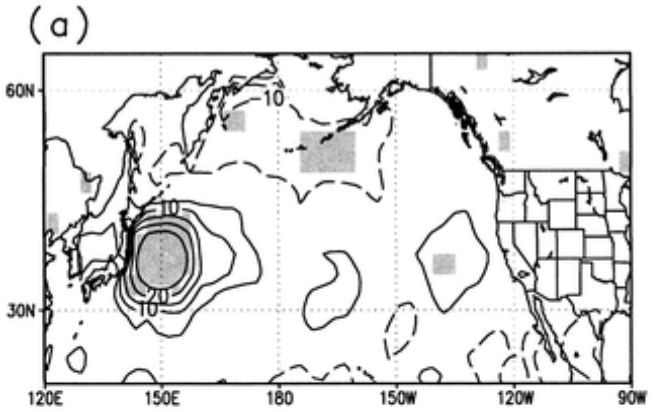

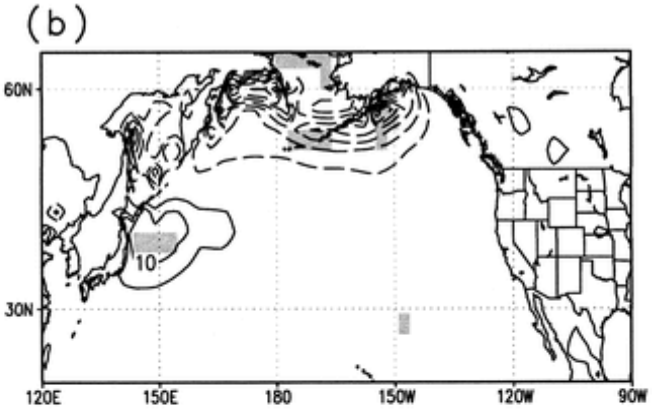

Sensible

Short wave

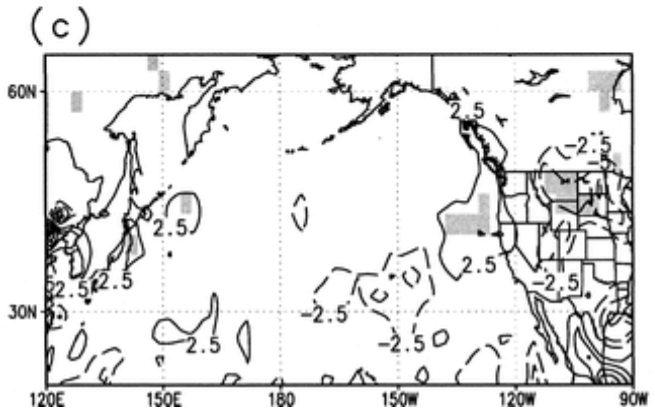

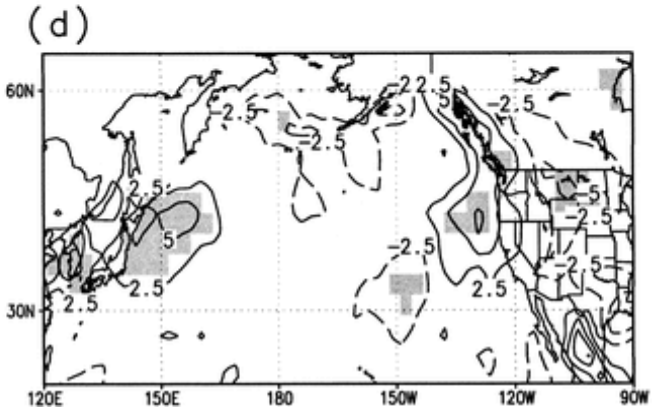

Long wave

Yulaeva et al. 2000

Response to ocean heat flux convergence in the KOE

SST

Wind stress

Q

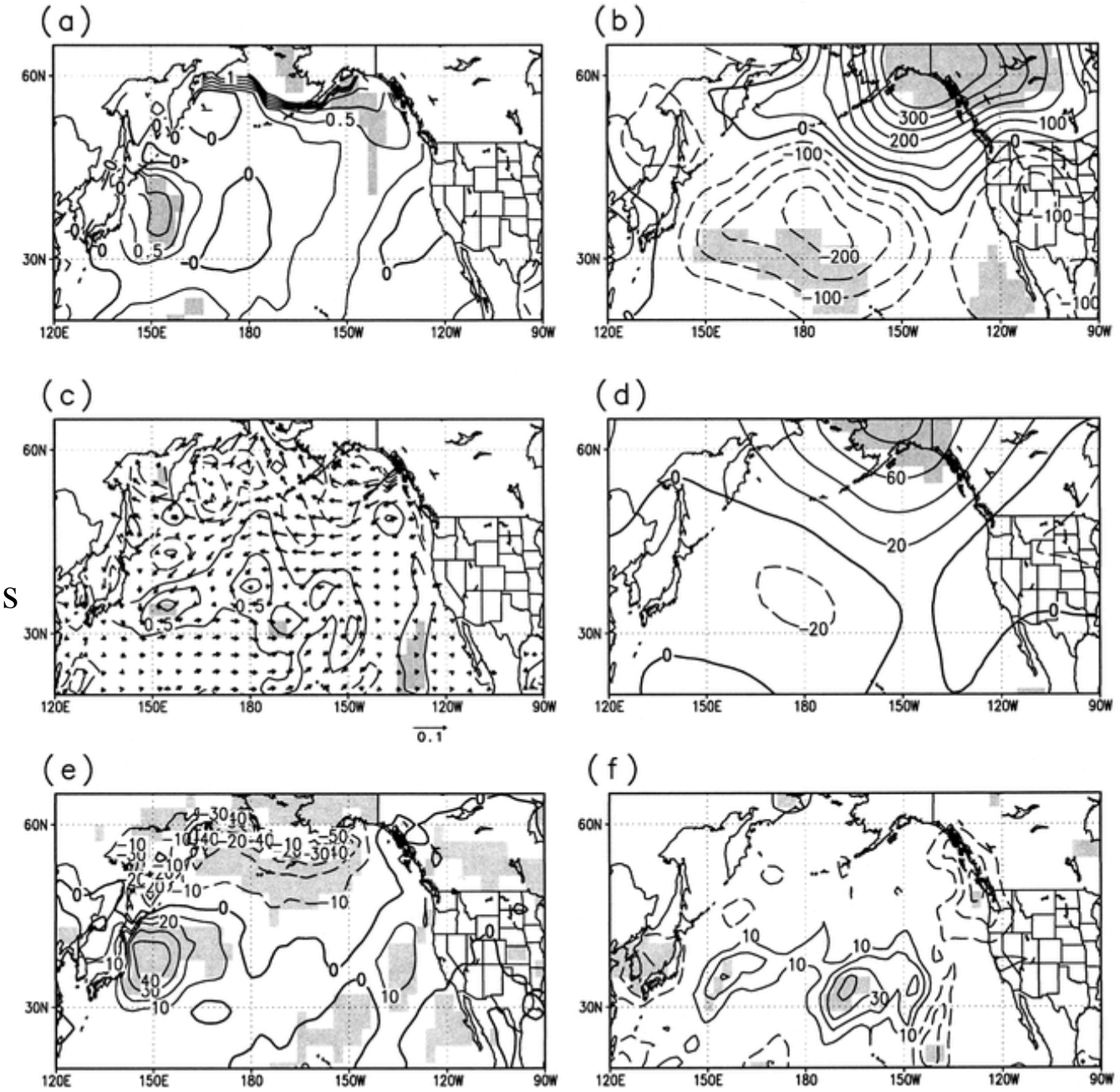

SLP/Pa

Z500/m

Precip.

Winter

Yulaeva et al. 2000

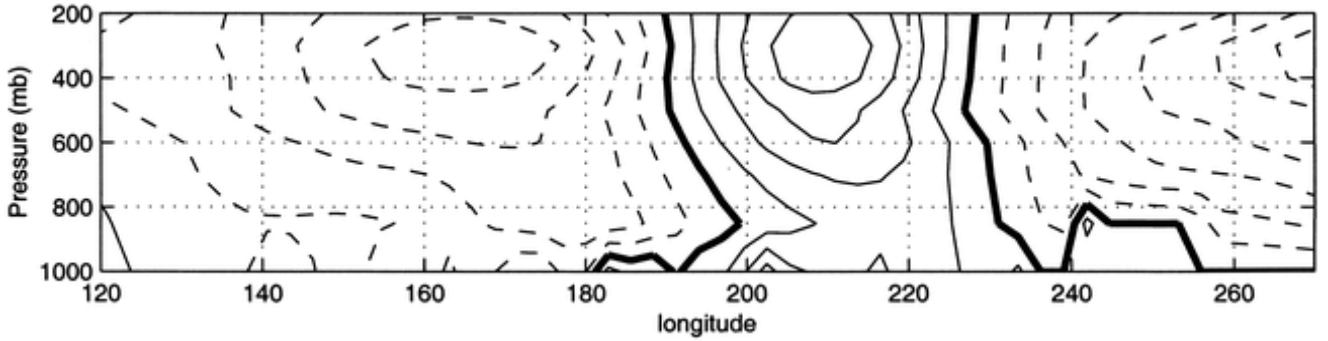

Response of Z500 at 40N, note the equivalent barotropic structure. Thus atmospheric eddy field provides essential physics. Contour interval 5m.

Yulaeva et al. 2000

Ocean heat flux response in the Atlantic

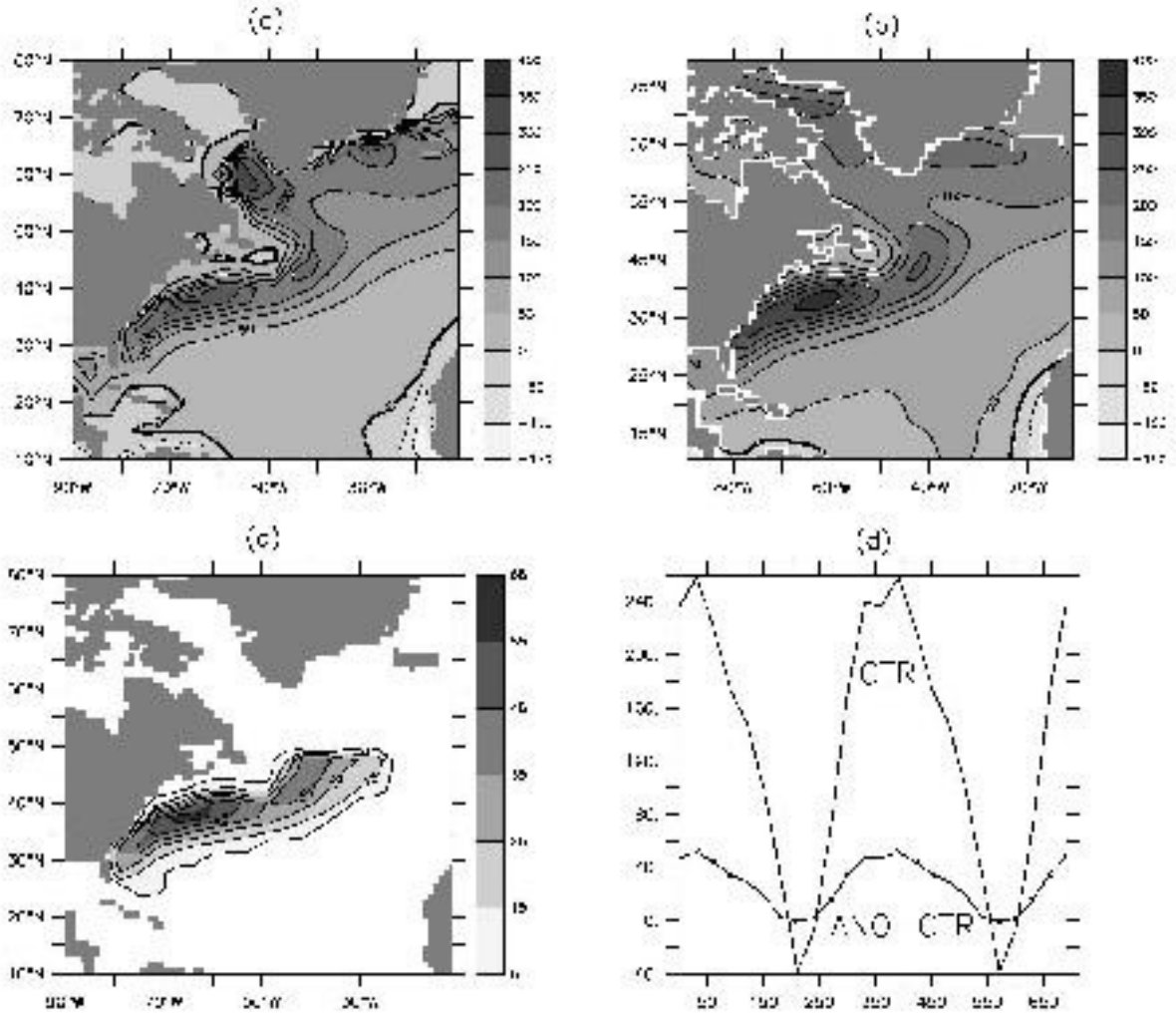

Figure 2. Ocean heat-flux convergence (OHFC) (W m^{-2}, positive upwards). (a) Annual mean of OHFC diagnosed from the calibration run, (b) annual mean of ocean–atmosphere heat flux from the da Silva *et al.* (1994) observational climatology, (c) January to March anomaly of OHFC, (d) temporal evolution of OHFC averaged between (60°W, 70°W) and (35°N, 45°N) for CTR (solid line) and ANO−CTR (crossed line).

Sutton and Mathieu 2002

SLP

Control

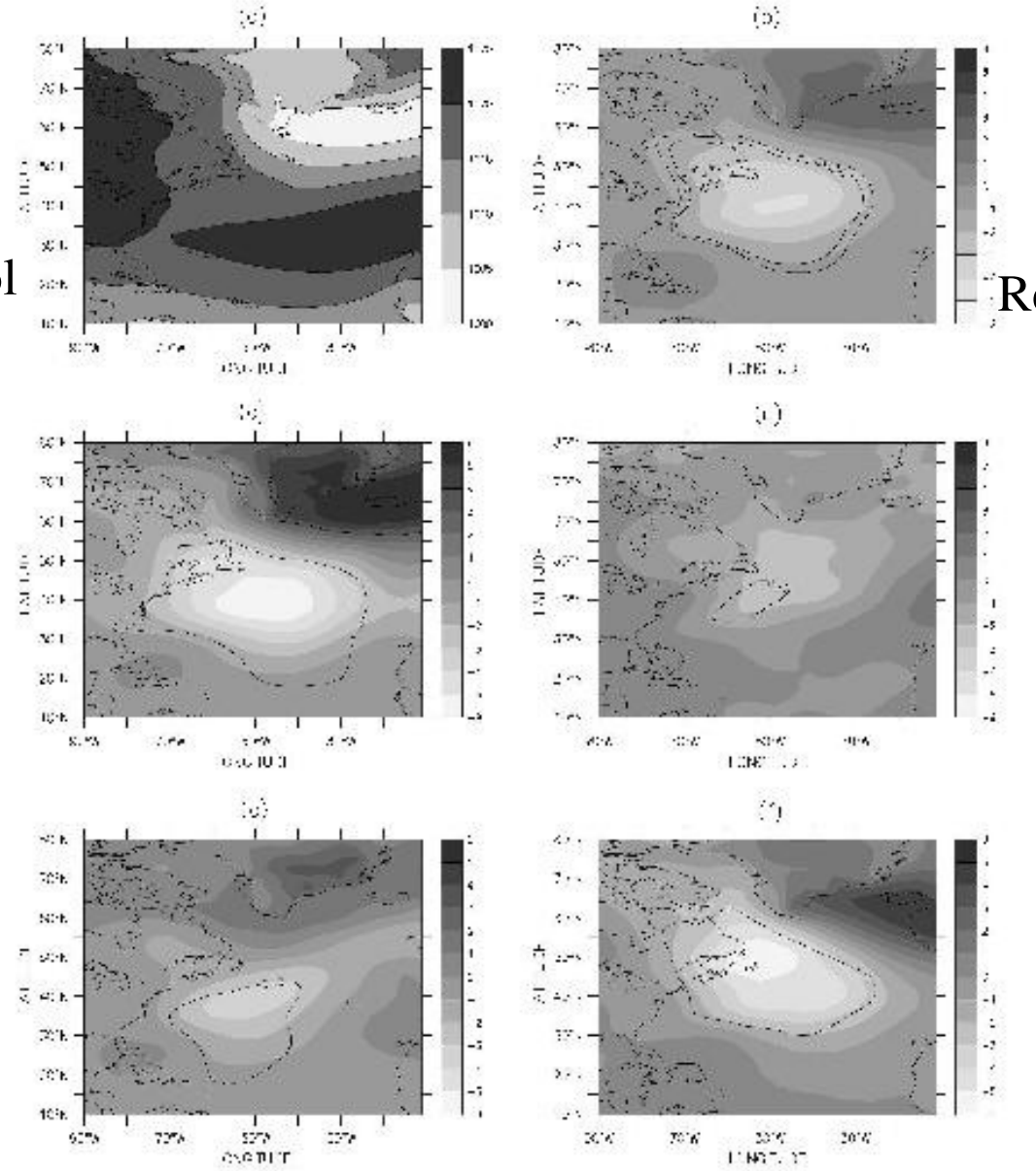

Responses

Figure 3. Winter response to ocean heat-flux convergence forcing as seen in sea-level pressure. (a) January to March average of ensemble-mean field (Pa) (experiment CTR); ensemble-mean anomaly (mb) (ANO−CTR) computed using (b) ten members, (c) five odd members (i.e. years 1, 3, 5, 7 and 9), (d) five even members (years 2, 4, 6, 8 and 10), (e) the first five members and (f) the last five members. The contours indicate where the response is statistically significant at the 90% (contour 0.1) or 95% (contour 0.05) confidence level.

Sutton and Mathieu 2002

Latent

Sensible

Long wave

Short wave

Net

SST

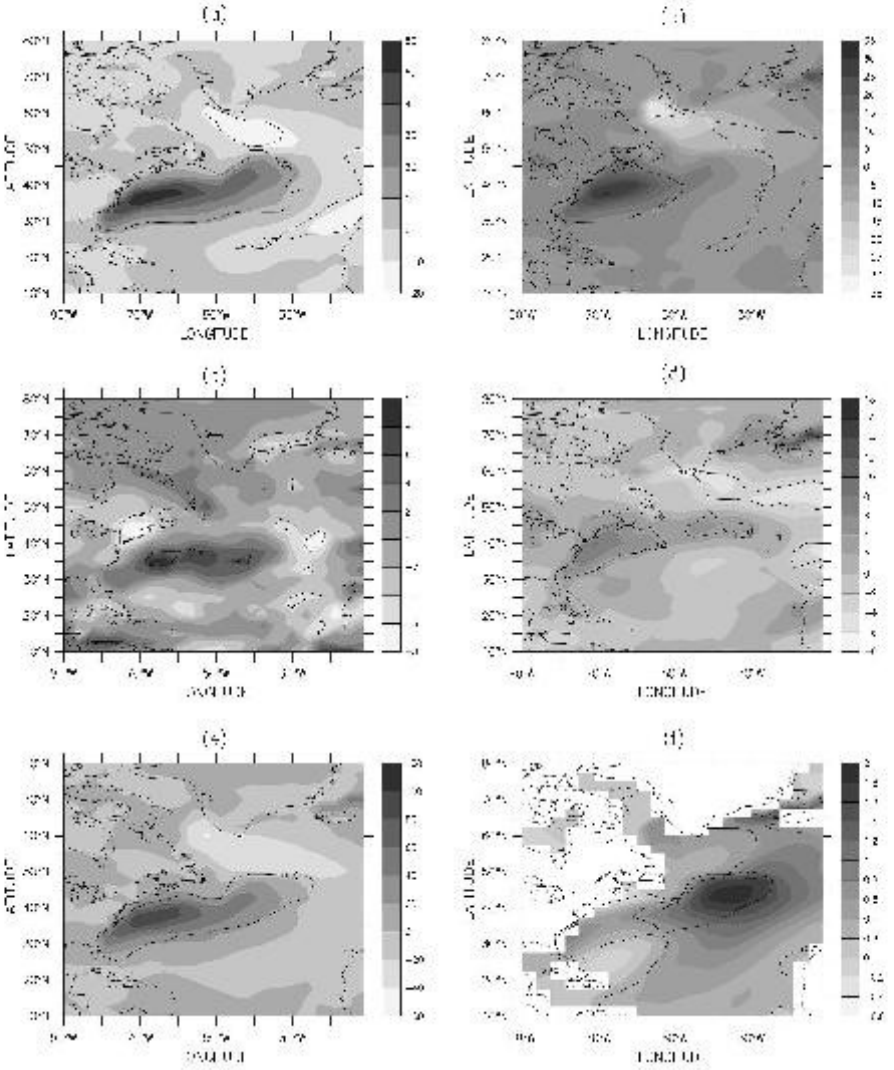

Figure 4. Winter response to ocean heat-flux convergence (OHFC) forcing as seen in air–sea heat flux (W m^{-2}) and sea surface temperature (SST) (°C). January to March average of ensemble-mean anomaly for (a) latent-heat flux, (b) sensible-heat flux, (c) long-wave radiation flux, (d) short-wave radiation flux, (e) net heat exchange, and (f) SST field. The contours in (a)–(d) indicate where the response is statistically significant at the 95% confidence level. The contour labelled 10.0 indicates the region where the OHFC forcing is applied.

Sutton and Mathieu

Generation of remote SST anomaly

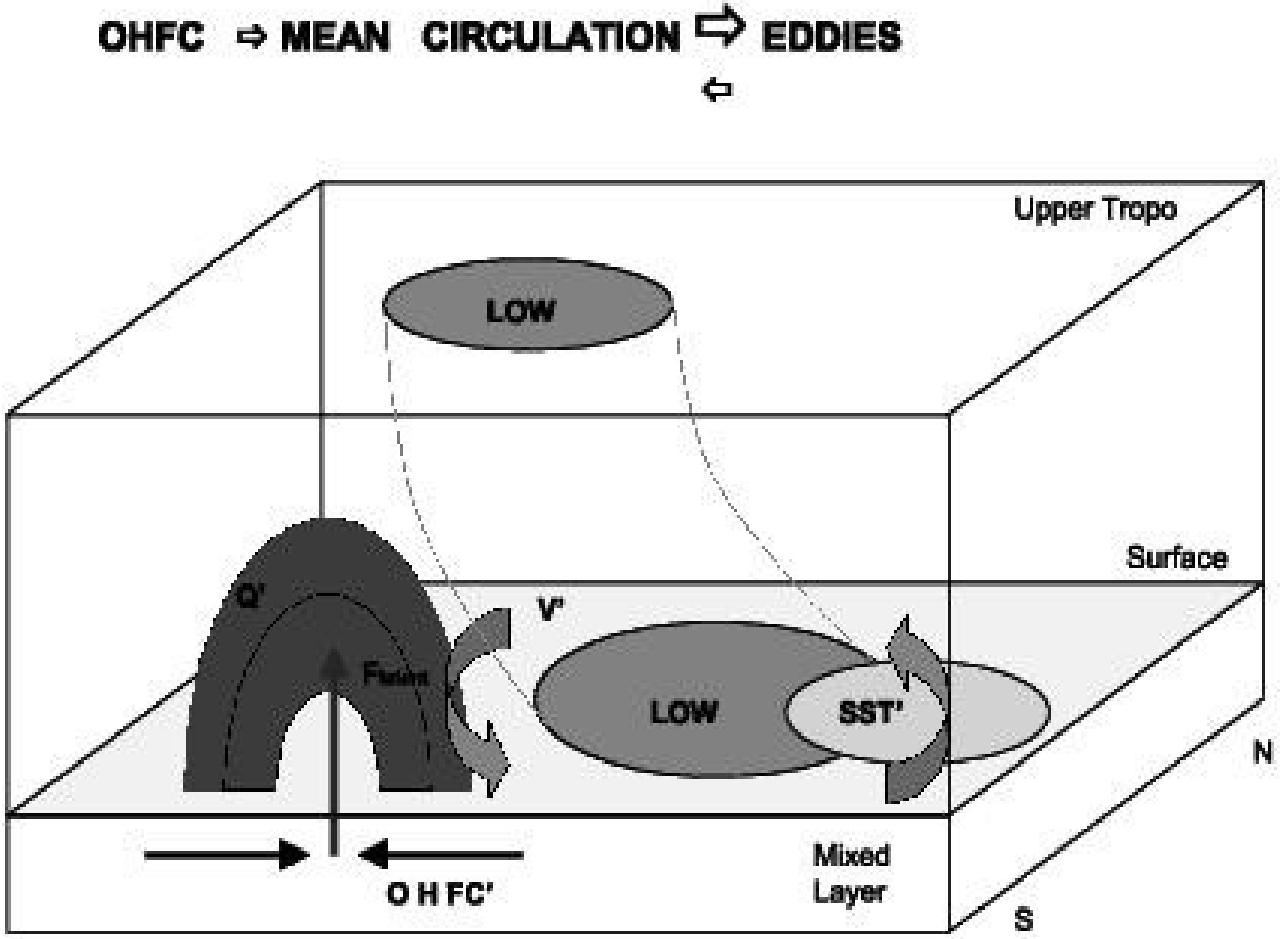

Figure 9. Schematic illustrating the response of the atmosphere–ocean mixed-layer system to an anomaly in ocean heat-flux convergence (OHFC). The OHFC forcing generates an anomalous air–sea flux exchange, particularly in the form of enhanced evaporation. Convergence in the atmosphere of this heat flux is associated with sensible and latent heating. The steady linear response to the heating is a Low downstream which tilts westwards with height. The anomalous low-level circulation balances the heating over the forcing region and also contributes to the formation of an sea-surface-temperature anomaly downstream. The changes in the time-mean tropospheric structure lead to changes in the transient eddies, but—in our experiment—these have a small effect back on the mean flow.

Sutton and Mathieu 2002